structure, drainage density and pattern of the Earth using remote sensor data. The chapter concludes with examples of how remote sensor data may be used to identify geomorphic features on the surface of the Earth.

Acknowledgments

The author wishes to thank the following people for their support and assistance in the preparation of this book. My wife, Marsha, provided patient encouragement during the years of manuscript preparation. Judith Berglund proof-read the manuscript and assisted in the preparation of the Appendix. Tim Ivey, a close friend, offered moral support. Dr. Susan Cutter provided resources and an environment within the Geography Department at the University of South Carolina that facilitated the creation of this book.

The author is indebted to the following scientists who reviewed selected chapters: Dr. John E. Estes, Dr. Glen Gustafson, Dr. Floyd Henderson, Dr. Chor Pang Lo, Dr. Jeff Luvall, Dr. Sunil Narumalani, Dr. Kevin Price, Dr. Dale Quattrochi, Dr. Don Rundquist, Judith Berglund, Jennifer Meisburger, and Steve Schill. Personnel at Prentice-Hall, Inc. were especially helpful including Dan Kaveney (Editor), Amanda Griffith (Assistant editor), and Ed Thomas (Production).

The American Society for Photogrammetry and Remote Sensing, the Association of American Geographers, Geocarto International Centre, Inc., American Elsevier Publishing Co., and Taylor & Francis, Inc. granted permission for the author to extract copyrighted material from his papers and other authors' works published in *Photogrammetric Engineering & Remote Sensing*, the *Manual of Remote Sensing, Manual of Color Aerial Photography, Annals* of the Association of American Geographers, *Geocarto International—A Multidisciplinary Journal of Remote Sensing & GIS, Professional Geographer, Remote Sensing of Environment, International Journal of Remote Sensing*, and *International Journal of Geographical Information Systems.*

John Pike of the Federation of American Scientists made available several useful remote sensing images. Large-scale kite aerial photography was provided by Dr. Cris Benton of the University of California Berkeley. Dr. Stefan Sandmeier of NASA Goddard provided much of the BRDF material. Several historical photographs were made available by the Harry Ransom Humanities Research Center, University of Texas, Austin, TX, and the Deutsches Museum, Munich, Germany.

A number of federal agencies were helpful, including: personnel of the Smithsonian National Air and Space Museum, the Library of Congress, National Aeronautics and Space Administration (NASA) Observatorium, NASA Goddard Tropical Rainfall Measurement Mission Office (Alan Nelson), NASA Goddard Solar and Heliospheric Observatory (Joseph Gurman), NASA John C. Stennis Space Center Commercial Remote Sensing Program (Dr. Bruce A. Davis), NASA Johnson Space Center (Dr. Kamlesh Lulla), NASA Marshall Space Flight Center (Dr. Dale Quattrochi), NASA Jet Propulsion Laboratory (JPL), U.S. Geological Survey (Don Lauer), USGS Desert Processes Working Group, USGS National Aerial Photography Program (NAPP), USGS Imaging Spectroscopy Lab (Roger Clark), National Oceanic and Atmospheric Administration (NOAA) and the Geological Survey of Canada.

Commercial remote sensing data providers made available examples of their remote sensing instruments and image products. A special thanks to: Space Imaging, Inc. (Linda Lidov), SPOT Image, Inc. (Clark Nelson), Lockheed Martin, Inc. (Jeannie Duisenberg and Eric Schulzinger), Litton Emerge Spatial, Inc. (Don Light), Positive Systems, Inc. (Kim Hickman), ORBIMAGE, Inc. (Sue Hale), EarthWatch, Inc., Intermap, Inc. (Ron Birk), Sovinformsputnik and Aerial Images, Inc. (Michele Hane), Aeromap USA, Inc., Environmental Research Institute of Michigan (Eric Kasischke), RADARSAT, Inc., Eastman Kodak Company (Robert Lundquist and Mary Skerrett), and Hughes Santa Barbara Research Center, Inc. Photogrammetric engineering firms provided information and images of their instruments, including: L-H Systems, Inc. (Dr. A. Stewart Walker), Marconi Integrated Systems, Inc. (Bob Hayes), E. Coyote Enterprises and Z/I Imaging, Inc. (Marilyn O'Cuilinn), Vexcel, Inc., Carl Zeiss, Inc. (Anke B. Shimko), and Optem, Inc. Digital image processing was performed using ERDAS and ENVI software. GIS analysis was performed using ESRI Arc-Info software.

John R. Jensen
University of South Carolina

Remote Sensing of the Environment 1

Scientists are concerned with observing nature, making careful observations and measurements, and then attempting to accept or reject hypotheses concerning these phenomena. The data collection may take place directly in the field (referred to as *in situ* or *in-place* data collection), or at some remote distance from the subject matter.

In Situ Data Collection

One form of *in situ* data collection involves the scientist going out in the field and questioning the phenomena of interest. For example, an enumerator for the decennial (10-year) census goes from door to door, asking people questions about their age, sex, education, income, etc. These data are recorded and used to document quantitatively the demographic characteristics of the population.

Conversely, a scientist may elect to use a *transducer* or other *in situ* measurement device at the study site to make measurements. Transducers are usually placed in direct physical contact with the object of interest. Many different types of transducers are available. For example, a scientist could use a thermometer to measure the temperature of the air, soil, or water; an anemometer to measure the speed of the wind; or a psychrometer to measure the humidity of the air. The data recorded by the transducers may be an analog electrical signal with voltage variations related to the intensity of the property being measured. Often these analog signals are transformed into digital values using analog-to-digital (A-to-D) conversion procedures. *In situ* data collection using transducers relieves the scientist of monotonous data collection often in inclement weather. Also, the scientist can distribute the transducers at important geographic locations throughout the study area, allowing the same type of measurement to be obtained at many locations at the same instant in time. Sometimes data from the transducers are telemetered electronically to a central collection point for rapid evaluation and archiving.

Two examples of *in situ* data collection are demonstrated in Figure 1-1. Leaf-area-index (LAI) measurements are being collected by a scientist at the study site using a handheld ceptometer in Figure 1-1a. Spectral reflectance measurements of the vegetation canopy are being obtained at the study site using a spectroradiometer in Figure 1-1b. LAI and spectral reflectance measurements obtained in the field may be used to calibrate LAI and spectral reflectance measurements collected by a remote sensing system located on an aircraft or satellite.

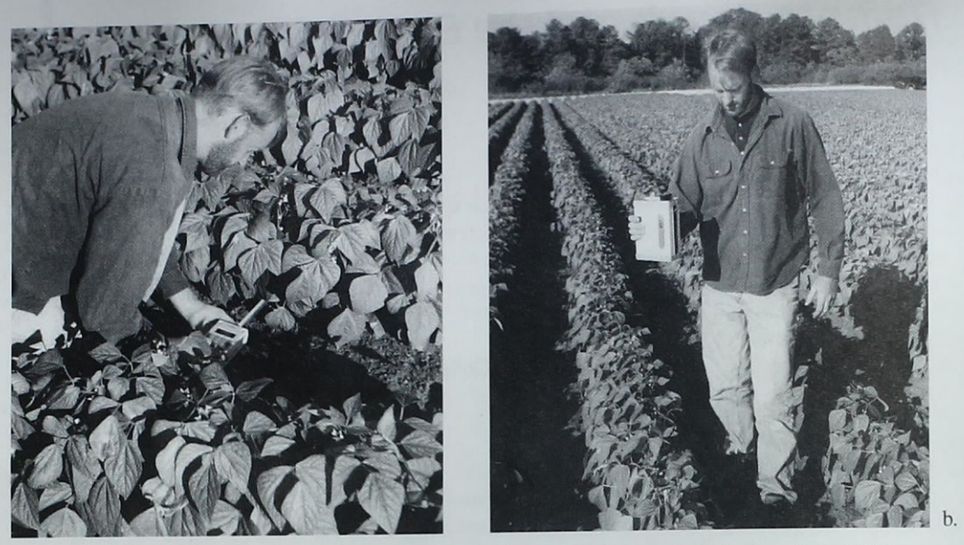

a. b.

Figure 1-1 *In situ* (in-place) data are collected in the field at the study site. a) A scientist is collecting leaf-area-index (LAI) measurements of soybeans (*Glycine max L. Merrill*) using a ceptometer that measures the number of "sunflecks" that pass through the vegetation canopy. The measurements are typically made above the canopy and on the ground below the canopy. The *in situ* LAI measurements may be used to calibrate LAI estimates derived from remote sensor data. b) Spectral reflectance measurements from the vegetation canopy are being collected using a spectroradiometer located 1 m above the canopy. The *in situ* spectral reflectance measurements may be used to calibrate the spectral reflectance measurements obtained from a remote sensing system onboard an aircraft or satellite.

Data collection by scientists in the field or by instruments placed in the field provide much of the data for physical, biological, and social science research. However, it is important to remember that no matter how careful the scientist is, error may be introduced during the *in situ* data-collection process. First, the scientist in the field can be *intrusive*. This means that unless great care is exercised, the scientist can actually change the characteristics of the phenomenon being measured during the data-collection process. For example, a scientist could lean out of a boat to obtain a surface-water sample from a lake. Unfortunately, the movement of the boat into the area may have stirred up the water column in the vicinity of the water sample, resulting in an unrepresentative, or *biased,* sample. Similarly, a scientist collecting a ceptometer LAI reading could inadvertently step on the sample site, compacting the vegetation canopy prior to data collection. Scientists may also collect data in the field using biased procedures. This introduces *method-produced error.* It could involve the use of a biased sampling design or the systematic, improper use of a piece of equipment. Finally, the *in situ* data-collection measurement device may be calibrated incorrectly. This can result in serious measurement error.

Intrusive *in situ* data collection, coupled with human method-produced error and measurement-device miscalibration, all contribute to *in situ* data-collection error. Therefore, it is a misnomer to refer to *in situ* data as *ground truth data.* Instead, we should simply refer to it as *in situ ground reference data*, acknowledging that it contains error.

Remote Sensing Data Collection

It is also possible to collect information about an object or geographic area from a distant vantage point (Figure 1-2) using specialized instruments (sensors). This remote data collection was originally performed using aerial cameras. *Photogrammetry* was defined in the early editions of the *Manual of Photogrammetry* as:

> "the art or science of obtaining reliable measurement by means of photography" (American Society of Photogrammetry, 1944; 1952; 1966).

Photographic interpretation is defined as:

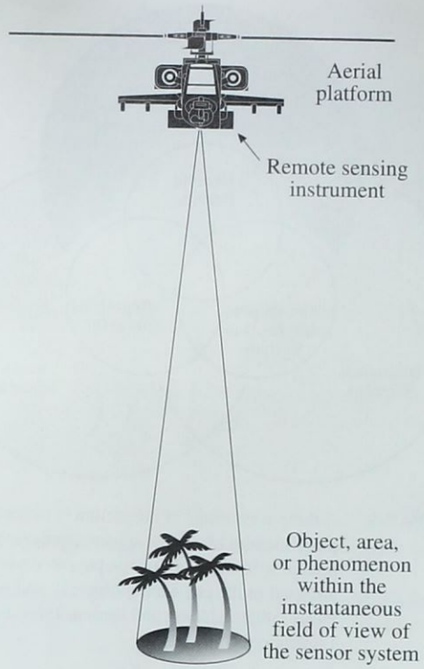

Figure 1-2 A remote sensing instrument collects information about an object or phenomenon within the instantaneous field of view of the sensor system without being in direct physical contact.

> "the act of examining photographic images for the purpose of identifying objects and judging their significance" (Colwell, 1960).

Remote sensing was formally defined by the American Society for Photogrammetry and Remote Sensing (ASPRS) as:

> *ASPRS Definition:* "the measurement or acquisition of information of some property of an object or phenomenon, by a recording device that is not in physical or intimate contact with the object or phenomenon under study" (Colwell, 1983).

In 1988, ASPRS adopted a combined definition of photogrammetry and remote sensing:

> *ASPRS Combined Definition:* "photogrammetry and remote sensing are the art, science, and technology of obtaining reliable information about physical objects and the environment, through the process of recording, measuring and interpreting imagery and digital representations of energy patterns derived from noncontact sensor systems" (Colwell, 1997).

But where did the term *remote sensing* come from? The actual coining of the term goes back to an unpublished paper in the early 1960s by the staff of the Office of Naval Research (ONR) Geography Branch (Pruitt, 1979; Fussell et al., 1986). Evelyn L. Pruitt was the author of the paper. She was assisted by staff member Walter H. Bailey. Aerial photo interpretation had become very important in World War II. The space age was just getting underway with the 1957 launch of *Sputnik* (U.S.S.R.), the 1958 launch of *Explorer 1* (U.S.), and the collection of photography from the then secret CORONA program initiated in 1960 (Table 1-1). In addition, the Geography Branch of ONR was expanding its research using instruments other than cameras (e.g., scanners, radiometers) and into regions of the electromagnetic spectrum beyond the visible and near-infrared regions (e.g., thermal infrared, microwave). Thus, in the late 1950s it had become apparent that the prefix "photo" was being stretched too far in view of the fact that the root word, *photography,* literally means "to write with [visible] light" (Colwell, 1997). Evelyn Pruitt (1979) wrote:

> "The whole field was in flux and it was difficult for the Geography Program to know which way to move. It was finally decided in 1960 to take the problem to the Advisory Committee. Walter H. Bailey and I pondered a long time on how to present the situation and on what to call the broader field that we felt should be encompassed in a program to replace the aerial photointerpretation project. The term 'photograph' was too limited because it did not cover the regions in the electromagnetic spectrum beyond the 'visible' range, and it was in these nonvisible frequencies that the future of interpretation seemed to lie. 'Aerial' was also too limited in view of the potential for seeing the Earth from space."

The term *remote sensing* was promoted in a series of symposia sponsored by ONR at the Willow Run Laboratories of the University of Michigan in conjunction with the National Research Council throughout the 1960s and early 1970s and has been in use ever since (Estes and Jensen, 1998).

Maximal/Minimal Definitions

Numerous other definitions of remote sensing have been proposed. In fact, Colwell (1984) suggests that "one measure of the newness of a science, or of the rapidity with which it is developing is to be found in the preoccupation of

its participating scientists with matters of terminology." Some have proposed an all-encompassing *maximal definition* where:

> *Maximal Definition:* "remote sensing is the acquiring of data about an object without touching it."

Such a definition is short, simple, general, and memorable. Unfortunately, it excludes little from the province of remote sensing (Fussell et al., 1986). It encompasses virtually all remote-sensing devices, including cameras, optical-mechanical scanners, linear and area arrays, lasers, radio-frequency receivers, radar systems, sonar, seismographs, gravimeters, magnetometers, and scintillation counters.

Others have suggested a more sharply focused, *minimalist definition* of remote sensing that adds qualifier after qualifier in an attempt to make certain that only legitimate functions are included in the term's definition. For example,

> *Minimal Definition:* "remote sensing is the noncontact recording of information from the ultraviolet, visible, infrared, and microwave regions of the electromagnetic spectrum by means of instruments such as cameras, scanners, lasers, linear arrays, and/or area arrays located on platforms such as aircraft or spacecraft, and the analysis of acquired information by means of visual and digital image processing."

Robert Green at NASA's Jet Propulsion Lab recently suggested we use the term *remote measurement* because data obtained using the new hyperspectral remote sensing systems are so accurate (Robbins, 1999). Each of the definitions are correct in an appropriate context. It is useful to briefly discuss components of these remote sensing definitions.

Remote Sensing: Art and/or Science?

Science: A *science* is defined as the broad field of human knowledge concerned with facts held together by *principles* (rules). Scientists discover and test these facts and principles by the scientific method, an orderly system of solving problems. Scientists generally feel that any subject that man can study by using the scientific method and other special rules of thinking may be called a science. The sciences include: 1) *mathematics* and *logic*, 2) the *physical sciences*, such as physics and chemistry, 3) the *biological sciences*, such as botany and zoology, and the 4) *social sciences*, such as geography, sociology, and anthropology (Figure 1-3). Interestingly, some persons do not consider mathematics and logic as sciences. But the fields of knowledge associated with

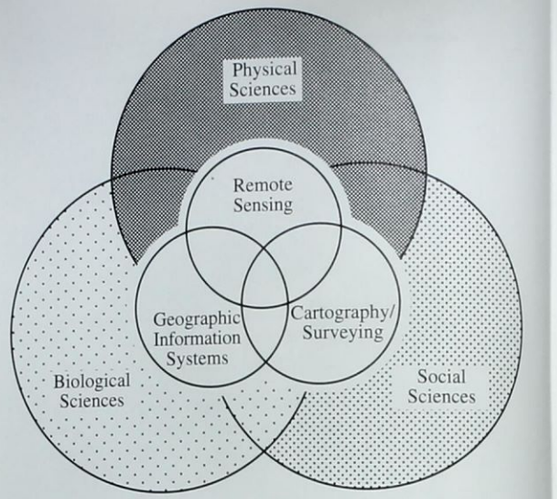

Figure 1-3 A three-way model of interaction between the mapping sciences of remote sensing, geographic information systems, and cartography/surveying as they are used in the physical, biological, and social sciences (after Dahlberg and Jensen, 1986; Fisher and Lindenberg, 1989).

mathematics and logic are such valuable *tools* for science that we cannot ignore them. Man's earliest questions were concerned with "how many" and "what belonged together." He struggled to count, to classify, to think systematically, and to describe exactly. In many respects, the state of development of a science is indicated by the use it makes of mathematics. A science seems to begin with simple mathematics to measure, then works toward more complex mathematics to explain.

Remote sensing is a tool or technique similar to mathematics. Using sophisticated sensors to measure the amount of electromagnetic energy exiting an object or geographic area from a distance and then extracting valuable information from the data using mathematically and statistically based algorithms is a *scientific* activity (Fussell et al., 1986). It functions in harmony with other *spatial* data-collection techniques or tools of the *mapping sciences*, including cartography and geographic information systems (GIS) (Fussell et al., 1986; Curran, 1987). In fact, Dahlberg and Jensen (1986) and Fisher and Lindenberg (1989) suggest a model where there is three-way interaction between remote sensing, cartography, and GIS, where no subdiscipline dominates and all are recognized as having unique yet overlapping areas of

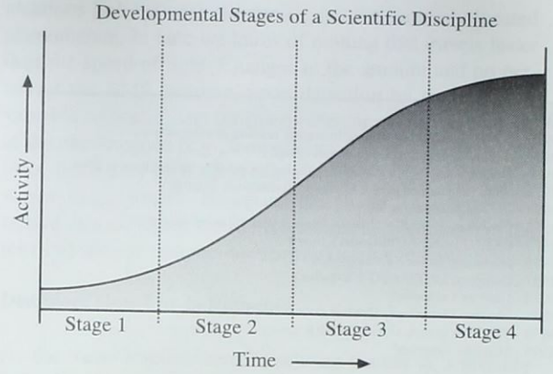

Figure 1-4 The developmental stages of a scientific discipline (adapted from Wolter, 1975; Jensen and Dahlberg, 1983).

knowledge and intellectual activity as they are used in physical, biological, and social science research (Figure 1-3).

The theory of science suggests that scientific disciplines go through four classic developmental stages. Wolter (1975) suggested that the growth of a discrete scientific discipline, such as remote sensing, that has its own techniques, methodologies, and intellectual orientation seems to follow the sigmoid or logistic curve illustrated in Figure 1-4. The growth stages of a scientific field are: Stage 1 — a preliminary growth period with small absolute increments of literature; Stage 2 — a period of exponential growth when the number of publications doubles at regular intervals; Stage 3 — a period when the rate of growth begins to decline but annual increments remain constant; and Stage 4 — a final period when the rate of growth approaches zero. The characteristics of a scholarly field during each of the stages may be briefly described as follows (Wolter, 1975): Stage 1 — little or no social organization; Stage 2 — groups of collaborators and existence of invisible colleges, often in the form of ad hoc institutes, research units, etc.; Stage 3 — increasing specialization and increasing controversy; and Stage 4 — decline in membership in both collaborators and invisible colleges.

Using this logic, it may be suggested that remote sensing is in Stage 2 of a scientific field, experiencing exponential growth since the mid-1960s with the number of publications doubling at regular intervals (Colwell, 1983; Cracknell and Hayes, 1993). Empirical evidence is presented in Table 1-1, including: 1) the organization of many specialized institutes and centers of excellence associated with remote sensing, 2) the organization of numerous professional societies devoted to remote sensing research, 3) the publication of numerous new scholarly remote sensing journals, 4) significant technological advancement such as improved sensor systems and methods of image analysis, and 5) intense self-examination. We are approaching Stage 3 with increasing specialization and theoretical controversy. However, the rate of growth of remote sensing has not begun to decline. In fact, there has recently been a tremendous surge in the numbers of persons specializing in remote sensing and commercial firms using remote sensing during the 1990s (Davis, 1999). Significant improvements in the spatial resolution of satellite remote sensing (e.g., more useful 1 x 1 m panchromatic data) is expected to bring even more social science GIS practictioners into the fold. Hundreds of new peer-reviewed remote sensing research articles are published every month.

Art: The process of visual photo or image interpretation brings to bear not only scientific knowledge but all of the background that a person has obtained through a lifetime. Such learning cannot be measured, programmed, or completely understood. The synergism of combining scientific knowledge with real-world analyst experience allows the interpreter to develop heuristic rules of thumb to extract valuable information from the imagery. It is a fact that some image analysts are much superior to other image analysts because they: 1) understand the scientific principles better, 2) are more widely traveled and have seen many landscape objects and geographic areas first-hand, and 3) they can synthesize scientific principles and real-world knowledge to reach logical and correct conclusions. Thus, remote sensing is both an art and a science.

Information About an Object or Area

Sensors can obtain very specific information about an object (e.g., the diameter of an oak tree crown) or the geographic extent of a phenomenon (e.g., the polygonal boundary of an entire oak forest). The electromagnetic energy emitted or reflected from an object or geographic area is used as a surrogate for the actual property under investigation. The electromagnetic energy measurements must be turned into information using visual and/or digital image processing techniques.

The Instrument (Sensor)

Remote sensing is performed using an instrument, often referred to as a *sensor*. The majority of remote sensing instruments described in this book record electromagnetic radiation (EMR) that travels at a velocity of 3×10^8 m s^{-1} from the source, directly through the vacuum of space or indirectly by reflection or reradiation to the sensor. The EMR represents an extremely efficient high-speed commu-

Table 1-1. Major Milestones in Remote Sensing

1600 and 1700s
1687 - Sir Isaac Newton's *Principia* summarizes basic laws of mechanics

1800s
1826 - Joseph Nicephore Niepce takes first photographic image
1839 - Louis M. Daguerre invents positive print daguerrotype photography
1839 - William Henry Fox Talbot invents Calotype negative/positive process
1855 - James Clerk Maxwell postulates additive color theory
1858 - Gaspard Felix Tournachon takes first aerial photograph from a balloon
1860s- James Clerk Maxwell develops electromagnetic wave theory
1867 - The term *photogrammetry* is used in a published work
1873 - Herman Vogel extends sensitivity of emulsion dyes to longer wavelengths, paving the way for near-infrared photography

1900
1903 - Airplane invented by Wright Brothers (Dec 17)
1903 - Alfred Maul patents a camera used to obtain photographs from a rocket.

1910s
1910 - International Society for Photogrammetry (ISP) founded in Austria
1913 - First International Congress of ISP in Vienna
1914 - 1918 World War I photo-reconnaissance

1920s
1920 - 1930 Increase in civilian use of photointerpretation and photogrammetry
1926 - Robert Goddard launches liquid-powered rocket (Mar 16)

1930s
1934 - American Society for Photogrammetry (ASP) founded
1934 - *Photogrammetric Engineering* (ASP)
1938 - *Photogrammetria* (ISP)
1939 - 1945 World War II photo-reconnaissance advances

1940s
1940s - Radar invented
1940s - Jet aircraft invented by Germany
1942 - Kodak patents first false-color infrared film
1942 - Launch of German V-2 rocket by Wernher VonBraun (Oct 3)

1950s
1950s - Thermal infrared remote sensing invented by military
1950 - 1953 Korean War aerial reconnaissance
1953 - *Photogrammetric Record* (Photogrammetric Society, U.K.)
1954 - Westinghouse, Inc. develops side-looking airborne radar system
1955 - 1956 U.S. Genetrix balloon reconnaissance program
1956 - 1960 Central Intelligence Agency U-2 aerial reconnaissance program
1957 - Soviet Union launched *Sputnik* satellite (Oct 4)
1958 - United States launched *Explorer 1* satellite (Jan 31)

1960s
1960s - Emphasis primarily on visual image processing
1960s - Michigan Willow Run Laboratory active — evolved into ERIM
1960s- *Intl. Symp. on Remote Sensing of Environment* (ERIM)
1960s - Purdue Lab for Agricultural Remote Sensing (LARS) active
1960s - Forestry Remote Sensing Lab at U.C. Berkeley (Robert Colwell)
1960s - ITC– Delft, initiates photogrammetric education for students worldwide
1960s - Digital image processing initiated at LARS, Berkeley, Kansas, ERIM
1960s - Declassification of radar and thermal infrared sensor systems
1960 - 1972 United States Corona spy satellite program
1960 - *Manual of Photointerpretation* (ASP)
1960 - *Remote sensing* term introduced by Office of Naval Research personnel
1961 - Yuri Gagarin becomes first human to travel in space
1961 - 1963 Mercury space program
1962 - Cuban Missile Crisis — U-2 photo-reconnaissance shown to the public
1964 - SR-71 discussed in President Lyndon Johnson press briefing
1965 - 1966 Gemini space program
1965 - *ISPRS Journal of Photogrammetry & Remote Sensing*
1969 - *Remote Sensing of Environment*, Elsevier

1970s
1970s, 80s - Possible to specialize in remote sensing at universities
1970s -Digital image processing comes of age
1970s -Remote sensing integrated with digital geographic information systems
1972 - ERTS-1 launched (Earth Resource Technology Satellite)
1973 - 1979 Skylab program
1973 - *Canadian Journal of Remote Sensing* (Canadian RS Society)
1975 - ERTS-2 launched (renamed Landsat 2)
1975 - *Manual of Remote Sensing* (ASP)
1977 - European METEOSAT-1 launched
1978 - Landsat 3 launched
1978 - Nimbus 7 launched - Coastal Zone Color Scanner
1978 - TIROS-N launched with AVHRR sensor
1978 - SEASAT launched

1980s
1980s - AAG Remote Sensing Specialty Group > 500 members
1980s - Commercialization attempted – EOSAT, Inc.
1980 - ISP becomes Intl. Soc. for Photogrammetry & Remote Sensing
1980 - *Intl. Journal of Remote Sensing* (Remote Sensing Society)
1980 - European Space Agency (ESA) created (Oct 30)
1980 - *IEEE Trans. Geoscience and Remote Sensing* (GRSS Society)
1981 - First *Intl. Geoscience and Remote Sensing Symposium*
1981 - NASA Space Shuttle program initiated (STS-1)
1981 - NASA Space Shuttle Imaging Radar (SIR - A) launched
1982 - Landsat 4 - Thematic Mapper and MSS launched
1983 - *Manual of Remote Sensing*, 2nd Ed. (ASP)
1983 - *Remote Sensing Reviews*
1984 - Landsat 5 - Thematic Mapper launched
1984 - NASA Space Shuttle Imaging Radar (SIR-B) launched
1986 - SPOT Image, Inc., launched SPOT 1
1986 - *Geocarto International* (Geocarto International Center)
1989 - *The Earth Observer* (NASA Goddard Space Flight Center)

1990s
1990s - Digital soft-copy photogrammetry comes of age
1990s - University degree programs in remote sensing available
1990s - NASA assists commercial use of remote sensing (Stennis Space Center)
1990s - Increased use of hyperspectral and LIDAR sensors
1990 - *Backscatter* (Alliance for Marine Remote Sensing Association)
1990 - SPOT Image, Inc., launched SPOT 2
1991 - NASA initiates "Mission to Planet Earth" (Goddard Space Flight Center)
1991 - European ERS-1 launched
1992 - U.S. Land Remote Sensing Policy Act becomes law
1993 - EOSAT Inc., Landsat 6 did not achieve orbit
1993 - SPOT Image, Inc., launched SPOT 3
1993 - NASA Space Shuttle Imaging Radar (SIR-C) launched
1995 - Canadian RADARSAT-1 launched
1995 - ERS-2 launched
1995 - Indian IRS-1C launched (5 x 5 m)
1995 - Corona imagery declassified, transferred to National Archives
1995 - *The Earth Observer* (EOS-Goddard)
1996 - *Manual of Photographic Interpretation*, 2nd Ed. (ASPRS)
1997 - *Addendum to Manual of Photogrammetry* (ASPRS)
1997 - EarthWatch, Inc., lost contact with Earlybird satellite
1998 - NASA MTPE redefined as "Earth Science Enterprise"
1998 - *Manual of Remote Sensing - Radar* (ASPRS)
1998 - SPOT Image, Inc., launched SPOT 4
1999 - *Manual of Remote Sensing - Geosciences* (ASPRS)
1999 - NASA Landsat 7 Enhanced Thematic Mapper Plus launched (April 15)
1999 - Space Imaging, Inc., IKONOS did not achieve orbit (Apr 27)
1999 - Space Imaging, Inc., launched a second IKONOS (Sept 24)
1999 - NASA *Terra* Earth observing system launched

2000 – 2001
2000 - NASA to initiate New Millennium Program
2000 - OrbView 3,4 to be launched by ORBIMAGE, Inc.
2000 - Quickbird to be launched by EarthWatch, Inc.
2001 - European Space Agency to launch Envisat

nications link between the sensor and the remotely located phenomenon. In fact, we know of nothing that travels faster than the speed of light. Changes in the amount and properties of the EMR become, upon detection by the sensor, a valuable source of data for interpreting important properties of the phenomenon (e.g., temperature, color). Other types of force fields may be used in place of EMR, including sound waves (e.g., sonar). However, the majority of remotely sensed data collected for Earth resource applications are the result of sensors that record electromagnetic energy.

Distance: How Far Is Remote?

As the name implies, remote sensing occurs at a distance from the object or area of interest. Interestingly, there is no clear distinction about how great this distance should be. The distance could be 1 meter, 100 meters, or > 1 million meters from the object or area of interest. In fact, virtually all astronomy is based on remote sensing. Many of the most innovative remote sensing systems and visual and digital image processing methods were originally developed for remote sensing extraterrestrial landscapes such as the moon, Mars, Io, Saturn, Jupiter, etc. Remote sensing science conducted by the Jet Propulsion Laboratory at the California Institute of Technology is particularly noteworthy. This text, however, is concerned primarily with remote sensing of the terrestrial Earth, using sensors that are placed on suborbital air-breathing aircraft, or orbital satellite platforms placed in the vacuum of space.

Remote sensing techniques may also be used to analyze inner space. For example, an electron microscope and associated hardware may be used to obtain photographs of extremely small objects on the skin, in the eye, etc. Similarly, an X-ray device is a remote sensing instrument where the skin and muscle are equivalent to the atmosphere that must be penetrated, and the interior bone or other matter is often the object of interest.

Remote Sensing Advantages and Limitations

Remote sensing has several unique advantages as well as some limitations.

Advantages

Remote sensing is *unobtrusive* if the sensor is passively recording the electromagnetic energy reflected from or emitted by the phenomenon of interest. This is a very important consideration, as passive remote sensing does not disturb the object or area of interest.

Remote sensing devices are often programmed to collect data systematically, such as within a single 9 x 9 in. frame of vertical aerial photography or a matrix (raster) of Landsat image data. This systematic data collection can remove the sampling bias introduced in some *in situ* investigations.

Under carefully controlled conditions, remote sensing can provide fundamental biophysical data, including: x,y location, z elevation or depth, biomass, temperature, moisture content, etc. In this sense it is much like surveying, providing fundamental data that other sciences can use when conducting scientific investigations. However, unlike much of surveying, the remotely sensed data may be obtained systematically over very large geographic areas rather than just single point observations.

Remote sensing is also different from the other mapping sciences such as cartography or GIS because they rely on data produced elsewhere. Remote sensing science yields fundamental scientific information. For example, a properly calibrated thermal infrared remote sensing system can provide a geometrically correct map of land- or sea-surface temperature without any other intervening science. In fact, remote sensing-derived information is now critical to the successful modeling of numerous natural (e.g., water-supply estimation; eutrophication studies; nonpoint source pollution) and cultural processes (e.g., land-use conversion at the urban fringe; water-demand estimation; population estimation) (Walsh et al., 1999). A good example is the digital elevation model that is so important in many spatially distributed GIS models. Digital elevation models are now produced almost exclusively through the analysis of remotely sensed data.

Limitations

Remote sensing science has limitations. Perhaps the greatest limitation is that its utility is often oversold. *It is not a panacea* that will provide all the information needed for conducting physical, biological, or social science. It simply provides some spatial, spectral, and temporal information of value.

Human beings select the most appropriate sensor to collect the data, specify the resolution of the data, calibrate the sensor, select the platform that will carry the sensor, determine when the data will be collected, and specify how the data are processed. Thus, human method-produced error may be introduced as the various remote sensing instrument and mission parameters are specified.

Powerful *active* remote sensor systems, such as lasers or radars that emit their own electromagnetic radiation, can be intrusive and affect the phenomenon being investigated.

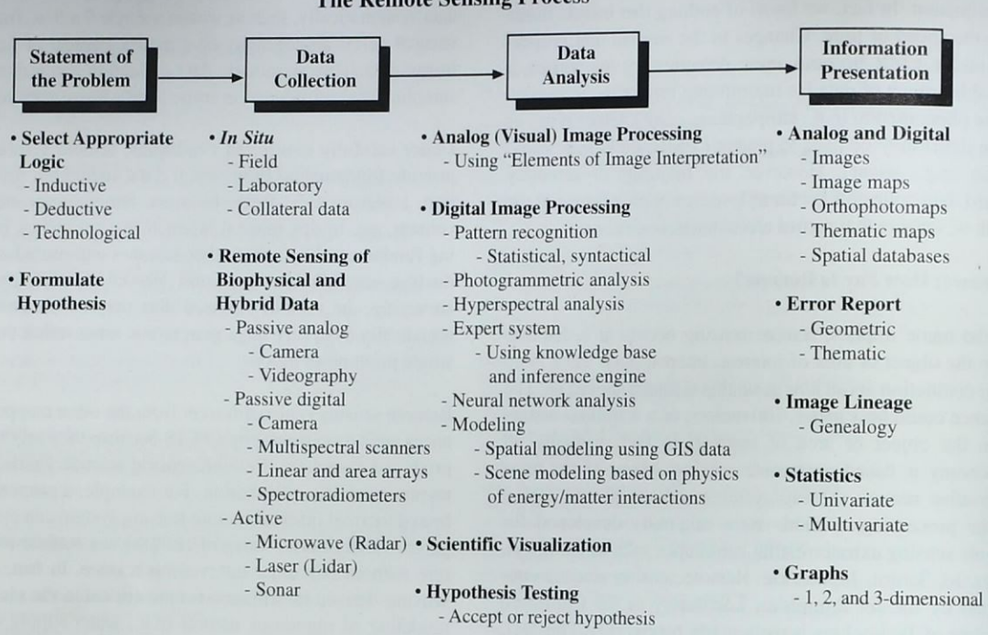

Figure 1-5 Scientists generally follow the remote sensing process when attempting to extract information from remotely sensed data.

Additional research is required to determine how intrusive these active sensors are.

Remote sensing instruments like *in situ* instruments often become uncalibrated, resulting in uncalibrated remote sensor data. Finally, remote sensor data may be expensive to collect and interpret or analyze. Hopefully, the information derived from the remote sensor data is of such value that the expense is warranted.

The Remote Sensing Process

Scientists have been developing procedures for collecting and analyzing remotely sensed data for more than 140 years. The first known photograph from an aerial platform (a tethered balloon) was obtained in 1858 by the Frenchman Gaspard Felix Tournachon (who called himself Nadar). Significant strides in aerial photography and other remote sensing data collection took place during World War I and II, the Korean conflict, the Cuban Missile Crisis, the Vietnam War, the Gulf War, and the war in Bosnia. Many of the accomplishments are summarized in Table 1-1 and in Chapter 3 (History of Aerial Photography and Aerial Platforms). Basically, military contracts to commercial companies resulted in the development of sophisticated electro-optical multispectral remote sensing systems and thermal infrared and microwave (radar) sensor systems whose characteristics are summarized in Chapters 7, 8, and 9, respectively. While the majority of the remote sensing systems may have been initially developed for military reconnaissance applications, the systems are also heavily used for monitoring the Earth's natural resources.

The remote sensing data-collection and analysis procedures used for Earth resource applications are often implemented in a systematic fashion that can be termed the *remote sensing process*. The procedures in the remote sensing process are summarized in Figure 1-5:

- statement of the problem,
- data collection,
- data analysis, and
- presentation of the information so that informed decisions can be made.

It is useful to review the characteristics of these procedures.

Statement of the Problem

The average man or woman and some children can look at aerial photography or other remote sensor data and extract some useful information from it. Generally, they do not interpret the images with any particular plan or hypothesis to test. Unfortunately, it is likely that they may make serious interpretation errors because they do not understand the nature of the remote sensing system used to acquire the data or appreciate the vertical or oblique perspective of the terrain recorded in the imagery.

Scientists who use remote sensing, however, are usually trained in the *scientific method* — a way of thinking about problems and solving them. The formal plan has at least five elements, including: 1) stating the problem, 2) forming the hypothesis (i.e., a possible explanation), 3) observing and experimenting, 4) interpreting data, and 5) drawing conclusions. It is not necessary to follow this formal plan exactly.

Three methodologies or types of logic may be used to structure the problem, such as (Curran, 1987):

- inductive logic,
- deductive logic, and/or
- technological logic.

Inductive logic involves observation, classification, generalization, and theory formulation. Inductive logic is used to build an objective description of observed facts or phenomena, which are then shaped and ordered to derive theory and thereby knowledge. Using inductive logic, the procedure starts with a large number of observations (n) that are true and hopefully unbiased. For example, we may observe on thousands of aerial images that:

> All healthy green mangrove forests appear red (magenta) on properly exposed color-infrared film.

Before such a theory can be considered legitimate, three conditions must be satisfied: 1) the number of observations must be large, 2) the observation must be repeated under a wide range of conditions, and 3) no accepted observation should *ever* conflict with the derived theory. The most serious limitation of inductive logic is that no number of apparently confirming observations can ever show that a theory is completely true.

The pursuit of knowledge using *deductive* logic has an emphasis not on observation but on the formulation of theory and the testing of hypotheses (Curran, 1987). Typically, the scientist states the problem and puts forth a speculative theory to solve that problem. He or she then puts forth a hypothesis (possible explanation). Observations are then made, often involving remote sensing imagery and *in situ* measurements made at unbiased locations. The null hypothesis is then tested at specific statistical confidence levels (e.g., 0.05 or 0.001). If the observations are such that the null hypothesis can be rejected, then the theory can be considered acceptable in the guarded sense that there is not an empirical basis for doubting its validity. If the observations do not support rejection (falsification) of the null hypothesis, then we must go back to our problem and evaluate other possible explanations that might lead to a falsifiable hypothesis.

For example, suppose we visited 100 mangrove forest sites in Florida and obtained color-infrared aerial photographs at each of the sites. We might develop the following null hypothesis:

> There is no significant relationship between healthy green mangrove forest and a red (magenta) appearance on properly exposed color-infrared film.

If the healthy green mangrove forest at 99 of the 100 sites did indeed have a red (magenta) appearance in the corresponding color-infrared film, then it would be possible for us statistically to reject (falsify) the null hypothesis. We could then state that there appears to be a statistically significant relationship between healthy green vegetation and the red (magenta) appearance on properly exposed color-infrared film. Unfortunately, there is a tendency to suggest that whenever a null hypothesis is not rejected, that either the sensor was not working properly or the ground reference data were in error, i.e., the observations are in doubt, not the theory. Fortunately, scientists wait until a theory is tested numerous times before it is accepted or rejected (Curran, 1987).

Some scientists extract new thematic information directly from remotely sensed imagery without ever explicitly using inductive or deductive logic. They are just interested in extracting information from the imagery using appropriate methods and technology. This *technological* approach is not as rigorous, but it is common in what some call *applied remote sensing*. The approach can also generate new knowledge.

Remote sensing is used in both scientific (inductive and deductive) and technological approaches to gain knowledge. There is debate as to how the different types of logic used in the remote sensing process and in GIS yield new scientific knowledge (e.g., Fussell et al., 1986; Curran, 1987; Fisher and Lindenberg, 1989; Ryerson, 1989; Duggin and Robinove, 1990; Dobson, 1993; Wright et al., 1997).

Identification of In Situ and Remote Sensing Data Requirements

If a hypothesis is formulated using deductive logic, a list of variables or observations are identified that will be used to verify or falsify the hypothesis. *In situ* observation and/or remote sensing may be used to collect information on the most important variables.

In Situ Data Requirements

Scientists using remote sensing technology should be well trained in field and laboratory data-collection procedures. For example, if a scientist wants to measure the surface temperature of a lake, it is usually essential that some accurate *in situ* lake-temperature measurements be obtained at the same time the remote sensor data are collected. These *in situ* observations may be used to 1) calibrate the remote sensor data, and 2) perform an unbiased accuracy assessment of the final results (Congalton and Green, 1998). Remote sensing textbooks provide some information on field and laboratory sampling techniques. The *in situ* sampling procedures, however, are learned best through formal courses in the sciences (e.g., chemistry, biology, forestry, soils, hydrology, meteorology). In addition, methods of collecting socioeconomic and demographic information in urban environments is often essential (e.g., cultural geography, sociology).

Most *in situ* data are now collected in conjunction with accurate x, y, z global positioning system (GPS) data (Jensen and Cowen, 1999). Scientists should know how to collect the fundamental GPS data and then perform differential correction to obtain the most accurate x, y, z coordinate information. Sometimes *collateral* data (often called *ancillary* data), such as soil maps, political boundary files, and block population statistics, collected by other scientists are of value in the remote sensing process. Ideally, these spatial collateral data reside in a digital GIS.

Usually it is necessary to collect both *in situ* and remotely sensed data because each type of data may be used to calibrate the other. For example, some *in situ* studies sample the environment and obtain county or statewide data such as population density. Remote sensing data can be used to disaggregate this sampled data. The spatial distribution of single- and multiple-family dwellings can be easily identified in high-resolution aerial photography. Such information may be used to disaggregate the population density within a county rather than assuming that the population is spread uniformly throughout the entire county. Similarly, a digital elevation model may be used to identify north-facing slopes and specific ranges of elevation (e.g., 1000 – 2000 m above sea level). Such information is very valuable when conducting a remote sensing vegetation study of mountainous terrain, where certain vegetation types only grow on north-facing slopes at an elevation of 1000 – 2000 m above sea level.

Remote Sensing Data Requirements

Once we have a list of variables, it is useful to determine those that can be remotely sensed. Remote sensing can provide information on two different classes of variables: *biophysical* and *hybrid*. Biophysical variables may be measured directly by the remote sensing system. This means that the remotely sensed data can provide fundamental biological and/or physical (*biophysical*) information directly, without having to use other surrogate or ancillary data. For example, a thermal infrared sensor can record the apparent temperature of a rock outcrop by measuring the radiant flux emitted from its surface. Similarly, it is possible to conduct remote sensing in a very specific region of the spectrum and identify the amount of water vapor in the atmosphere. It is also possible to measure soil moisture content directly using microwave remote sensing techniques (Engman and Chauhan, 1995). All three of these are true biophysical measurements. Such data are useful in physical science models.

Another example is the determination of the precise x, y location and height (z) of an object. Such information can be extracted directly from stereoscopic aerial photography, overlapping satellite imagery (e.g., SPOT) or interferometric radar imagery. A list of selected biophysical variables that can be remotely sensed and useful sensors to acquire such data are found in Table 1-2. The characteristics of most of these sensor systems are discussed in Chapters 7, 8, and 9. Great strides have been made in remotely sensing many of these biophysical variables (Eidenshink, 1992; ESA, 1992). They are important to the national and international effort under way to model the global environment (Lousma, 1993; Asrar and Dozier, 1994; Jones et al.,1997).

The second general group of variables that may be remotely sensed include *hybrid* variables, created by systematically analyzing more than one biophysical variable. For example, by remotely sensing a plant's chlorophyll absorption characteristics, temperature, and moisture content, it may be possible to model these data to detect vegetation stress, a hybrid variable. The variety of hybrid variables is large; consequently, no attempt is made to identify them. It is important to point out, however, that nominal-scale land-cover mapping is a hybrid variable. The land cover of a particular area on an image is usually derived by evaluating several of the fundamental biophysical variables at one time [e.g., object tone or color, location (x, y), height (z), and perhaps temper-

Table 1-2. Biophysical and Hybrid Variables and Potentially Useful Remote Sensing Systems (proposed sensor systems are in italics)

Biophysical Variables	Potential Remote Sensing System
***x, y* Geographic location**	Aerial photography, Landsat TM, SPOT HRV, Russian KVR-1000, IRS-1CD, ATLAS, Radarsat, ERS-1,2 microwave, Landsat 7 ETM+, Space Imaging IKONOS, Terra *MODIS, ASTER, EarthWatch Quickbird, ORBIMAGE OrbView 3,4*
***z* Topographic/bathymetric**	Aerial photography, TM, SPOT, IRS-1CD, Radarsat, LIDAR systems, ETM, IKONOS, *ASTER, Quickbird, OrbView 3,4*
Vegetation chlorophyll concentration biomass (green & dead) foliar water content Absorbed photosynthetically active radiation phytoplankton	 Air photos, TM, SPOT, IRS-1CD, ETM, IKONOS, *ASTER, MODIS, OrbView 3,4* Air photos, AVHRR, TM, SPOT, IRS-1CD, ETM, IKONOS, *MODIS, OrbView 3,4* Radarsat, ERS-1,2; TM Mid-IR, ETM, IKONOS, *MODIS, ASTER, OrbView 3,4* ETM, IKONOS, *MODIS, OrbView 3,4* SeaWiFS, TM, AVHRR, ETM, IKONOS, *MODIS, OrbView 3,4*
Surface temperature	GOES, SeaWiFS, AVHRR, TM, Daedalus, ATLAS, ETM, *ASTER, MODIS*
Soil moisture	ALMAZ, TM, ERS-1,2; Radarsat, Intermap Star 3i, IKONOS, *ASTER, OrbView 3,4*
Surface roughness	Air photos, ALMAZ, ERS-1,2; Radarsat, Star 3i, IKONOS, *ASTER, OrbView 3,4*
Evapotranspiration	AVHRR, TM, SPOT, CASI, ETM, *MODIS, ASTER*
Atmosphere tropospheric chemistry, temperature, water vapor, wind speed/direction, energy inputs, precipitation, cloud and aerosol properties	GOES, UARS, ATREM, *MODIS, MISR, CERES, MOPITT*
BRDF (bidirectional reflectance distribution function)	*MODIS, MISR, CERES*
Ocean color, phytoplankton, biochemistry, sea height	TOPEX/POSEIDON, SeaWiFS, ETM, IKONOS, *MODIS, MISR, ASTER, CERES, OrbView 3,4*
Snow and sea ice extent and characteristics	Aerial photography, AVHRR, TM, SPOT, Radarsat, SeaWiFS, IKONOS, ETM, *MODIS, ASTER, OrbView 3,4; Quickbird*
Volcanic effects temperature, gases	ATLAS, *MODIS, MISR, ASTER*
Selected Hybrid Variables	**Potential Remote Sensing System**
Land use urban infrastructure and land use	Aerial photography, AVHRR, TM, SPOT, Russian KVR-1000, IRS-1CD, Radarsat, Star 3i, ETM, IKONOS, *MODIS, ASTER, OrbView 3,4; Quickbird*
Vegetation stress	Aerial photography, Daedalus, ATLAS, AVHRR, TM, SPOT, IRS-1CD, IKONOS, SeaWiFS, ETM, *MODIS, ASTER, OrbView 3,4; Quickbird*

ature]. So much attention has been placed on remotely sensing this hybrid *nominal*-scale variable that the *interval*- or *ratio*-scaled biophysical variables have been neglected until the last decade. Nominal-scale land-use mapping is an important capability of remote sensing technology and should not be minimized. In fact, many social and physical scientists routinely use such data in their research. However, we now see a dramatic increase in the extraction of interval- and ratio-scaled biophysical data that are so valuable when incorporated into quantitative models that can accept spatially distributed information (e.g., Asrar and Dozier, 1994; Moran et al., 1997; NASA, 1998).

Remote Sensing Data Collection

Remotely sensed data are collected using either passive or active remote sensing systems. *Passive* sensors record naturally occurring electromagnetic radiation that is reflected or emitted from the terrain. For example, cameras and video recorders may be used to record visible and near-infrared energy reflected from the terrain, and a multispectral scanner may be used to record the amount of thermal radiant flux emitted from the terrain. *Active* sensors such as microwave (radar) or sonar bathe the terrain in man-made electromagnetic energy and then record the amount of radiant flux scattered back toward the sensor system.

Remote sensing systems collect analog (e.g., hard-copy aerial photography or video data) and/or digital data [e.g., a matrix (raster) of brightness values obtained using a scanner, linear array, or area array]. A selected list of some of the most important current and proposed remote sensing systems is presented in Table 1-3.

Sensor Resolution

Each remote sensing system has four major resolutions associated with it. These resolutions should be understood by the scientist in order to extract meaningful biophysical or hybrid information from the remotely sensed imagery. *Resolution* (or resolving power) is defined as a measure of the ability of an optical system to distinguish between signals that are spatially near or spectrally similar.

Spectral Resolution: This refers to the number and dimension of specific wavelength intervals in the electromagnetic spectrum to which a remote sensing instrument is sensitive. The Landsat Multispectral Scanner (MSS) provided a tremendous amount of remotely sensed data of much of the Earth which is still of significant value for historical studies. The bandwidths of the four MSS bands are displayed in Figure 1-6a (band 1 = 0.5 – 0.6 μm; band 2 = 0.6 – 0.7 μm; band 3 = 0.7 – 0.8 μm; and band 4 = 0.8 – 1.1 μm). The nominal size of a band may be large (i.e., coarse), as with the Landsat MSS near-infrared band 4 (0.8 – 1.1 μm) or relatively smaller (i.e., finer), as with the Landsat MSS band 3 (0.7 – 0.8 μm). Thus, Landsat MSS band 4 detectors record a relatively large range of reflected near-infrared radiant flux (300 nm) while the MSS band 3 detectors record a much reduced range of near-infrared radiant flux (100 nm).

The four spectral bandwidths associated with the Positive Systems, Inc. ADAR 5500 digital frame camera are shown for comparative purposes (Figure 1-6a). The frame camera's bands are refined to record information in more specific regions of the electromagnetic spectrum (band 1 = 450 – 515 nm; band 2 = 525 – 605 nm; band 3 = 640 – 690 nm; and band 4 = 750 – 900 nm). In fact, there are gaps in the spectral sensitivity of the detectors. Note that this digital camera system is also sensitive to reflected blue wavelength energy.

The aforementioned terminology is typically used to describe a sensor's *nominal spectral resolution*. Unfortunately, it is difficult to create a detector that has extremely sharp bandpass boundaries such as those shown in Figure 1-6a. Rather, the more precise method of stating bandwidth is to look at the typical Gaussian-shape of the detector sensitivity, such as the example shown in Figure 1-6b. The analyst then determines the Full Width at Half Maximum (FWHM). In this hypothetical example, the Landsat MSS near-infrared band 3 under investigation is sensitive to energy between 0.7 and 0.8 µm (700 – 800 nm).

Remote sensing systems may be configured to collect data in just a single band or region of the electromagnetic spectrum. For example, an ADAR 5500 band 4 near-infrared image is displayed in Figure 1-6c. *Multispectral* remote sensing takes place when radiant energy is recorded in multiple bands of the electromagnetic spectrum. The ADAR 5500 usually acquires four multispectral bands of imagery during a mission (Figure 1-6d). A *hyperspectral* remote sensing instrument acquires data in hundreds of spectral bands. For example, the Airborne Visible and Infrared Imaging Spectrometer (AVIRIS) has 224 bands in the region from 0.4 – 2.5 μm spaced just 10 nm apart based on the FWHM criteria (Clark, 1999). An AVIRIS hyperspectral datacube of Sullivan's Island, SC, is shown in Figure 1-7.

Certain regions or bands of the electromagnetic spectrum are optimum for obtaining information on biophysical parameters. The bands are normally selected to maximize the con-

Table 1-3. Selected Current and Proposed Remote Sensing Systems and their Major Characteristics

Remote Sensing Systems	Resolution: Spectral: Blue	Green	Red	Near-IR	Mid-IR	Thermal IR	Microwave	Spatial (meters)	Temporal (days)
Suborbital Sensors									
Panchromatic film (b&w)	0.5 ——— 0.7 µm							Variable	Variable
Color film	0.4 ——— 0.7 µm							Variable	Variable
Color-infrared film	0.5 ——— 0.9 µm							Variable	Variable
NASA Airborne Terrestrial Applications Sensor (ATLAS)	0.45 ——— 8 bands ——— 2.35 µm					6	—	2.5 to 25	Variable
NASA Airborne Visible IR Imaging Spectrometer (AVIRIS)	0.41 ——— 224 bands ——— 2.5 µm							2.5 or 20	Variable
Intermap Star-3i X-band radar							1	Variable	Variable
Satellite Sensors									
NOAA-9 AVHRR LAC	—	—	1	1	—	3	—	1100	14.5/day
NOAA- K, L, M (proposed)	—	—	1	1	2	2	—	1100	14.5/day
Landsat Multispectral Scanner (MSS)	—	1	1	2	—	—	—	79	16–18
Landsat 4-5 Thematic Mapper (TM)	1	1	1	1	2	1	—	30 and 120	16
Landsat 7 Enhanced TM (ETM+) — Multispectral	1	1	1	1	2	1	—	30 and 60	16
— Panchromatic	—	0.52 ——— 0.9 µm			—	—	—	15	16
SPOT HRV — Multispectral	—	1	1	1	—	—	—	20	Pointable
— Panchromatic		0.51 ——— 0.73 µm			—	—	—	10	Pointable
GOES Series (East and West)	—	0.52 ——— 0.72 µm			—	4	—	700	0.5/hr
European Remote Sensing Satellite (ERS-1,2)	VV polarization C-band (5.3 GHz)						1	26 – 28	—
Canadian RADARSAT (several modes)	HH polarization C-band (5.3 GHz)						1	9 to 100	1–6 days
Shuttle Imaging Radar (SIR-C)	—	—	—	—	—	—	3	30	Variable
Sea-Viewing Wide Field-of-View Sensor (SeaWiFS)	3	2	1	2	—	—	—	1130	1
Terra Moderate Resolution Imaging Spectrometer (*MODIS*)	0.405 ——— 36 bands ——— 14.385 µm						—	250, 500, 1000	1-2
Terra Advanced Spaceborne Thermal Emission and Reflection Radiometer (*ASTER*)	0.52 — 3 bands — 0.86 µm							15	5
					1.6 – 6 bands – 2.43 µm			30	16
					8.12 – 5 bands – 11.6 µm			90	16
Terra Multiangle Imaging SpectroRadiometer (*MISR*)	Nine CCD cameras in four bands (440, 550, 670, 860 nm)							275 and 1100	
NASA Topex/Poseidon — TOPEX radar altimeter	(18, 21, 37 GHz)							315 km	10
— POSEIDON single-frequency radiometer	(13.65 GHz)								
NASA Upper Atmosphere Research Satellite (UARS): includes 9 sensors.									
Space Imaging IKONOS — Multispectral	1	1	1	1			—	4	Pointable
— Panchromatic	0.45 ——— 0.9 µm					—	—	1	
ORBIMAGE Orbview 3 — Multispectral	1	1	1	1			—	4	Pointable
— Panchromatic	0.45 ——— 0.9 µm				—	—	—	1	

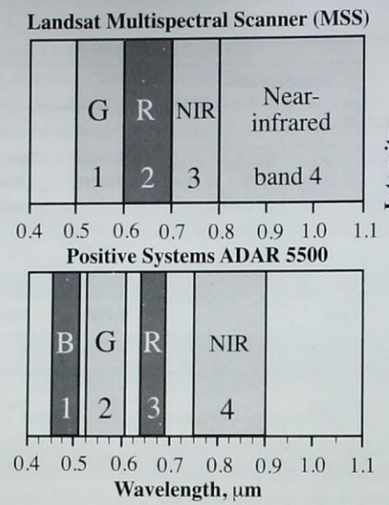

a. Nominal spectral resolution of the Landsat Multispectral Scanner and Positive Systems ADAR 5500 digital frame camera.

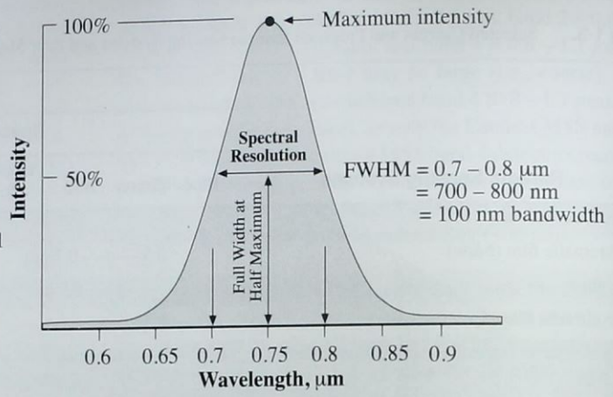

b. Precise bandpass measurement of a detector based on Full Width at Half Maximum (FWHM) criteria

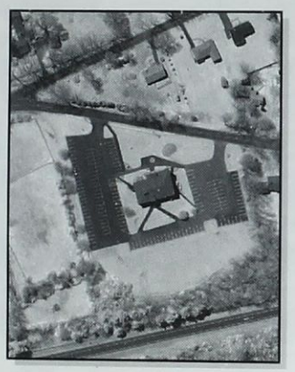

c. Single band of ADAR 5500 data

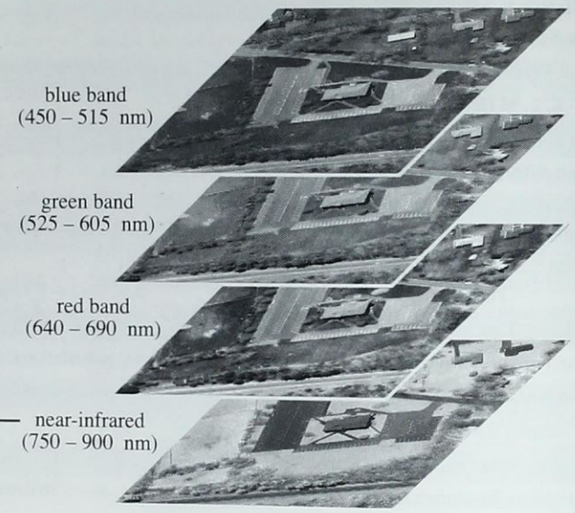

d. Multispectral remote sensing

Figure 1-6 a) The spectral bandwidths of the four Landsat Multispectral Scanner (MSS) bands (green, red, and two near-infrared) compared with the bandwidths of the Positive Systems ADAR 5500 digital frame camera. b) The true spectral bandwidth is the width of the Gaussian-shaped spectral profile at Full Width at Half Maximum (FWHM) intensity (after Clark, 1999). This example has a spectral bandwidth of 0.1 μm (100 nm) between 700 and 800 nm. c) If desired, it is possible to collect reflected energy in a single band of the electromagnetic spectrum (e.g., 750 – 900 nm). d) Multispectral remote sensing instruments such as the ADAR 5500 collect data in multiple bands of the electromagnetic spectrum (images courtesy of Positive Systems, Inc.).

Airborne Visible Infrared Imaging Spectrometer (AVIRIS) Datacube of Sullivan's Island, SC, Obtained on October 26, 1998

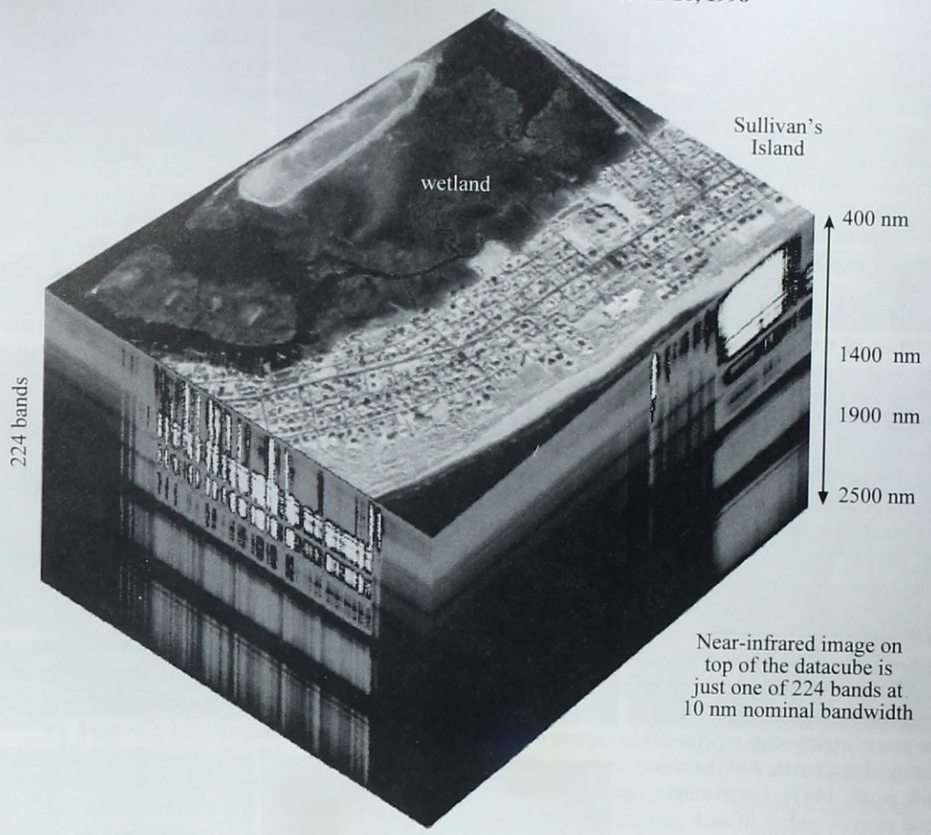

Near-infrared image on top of the datacube is just one of 224 bands at 10 nm nominal bandwidth

Figure 1-7 Hyperspectral remote sensing of Sullivan's Island, SC, on October 26, 1998, using NASA's Airborne Visible Infrared Imaging Spectrometer (AVIRIS). The spatial resolution is 2.5 x 2.5 m. The atmosphere absorbs most of the electromagnetic energy near 1.4 and 1.9 μm (Meisburger and Jensen, 1999; datacube courtesy of NASA Jet Propulsion Laboratory).

trast between the object of interest and its background (i.e., object-to-background contrast). Careful selection of the spectral bands may improve the probability that a feature will be detected and identified and biophysical information extracted.

Spatial Resolution: There is a relationship between the size of a feature to be identified and the spatial resolution of the remote sensing system. *Spatial resolution* is a measure of the smallest angular or linear separation between two objects that can be resolved by the sensor. The spatial resolution of aerial photography may be measured by 1) placing carefully calibrated, parallel black-and-white lines on tarps that are placed in the field, 2) obtaining aerial photography of the study area, and 3) analyzing the photography and computing the number of resolvable *line pairs per millimeter* in the photography. It is also possible to determine the spatial resolution of imagery by computing its modulation transfer function, which is beyond the scope of this text.

Many satellite remote sensing systems operate in fixed orbits with fixed optical systems that have a constant instantaneous-field-of-view (IFOV). For practical purposes, therefore, we define a sensor system's nominal spatial resolution as simply the dimension in meters (or feet) of the ground-projected IFOV. For example, the SPOT panchromatic band has a nominal spatial resolution of 10 x 10 m, the Landsat Thematic Mapper has a nominal spatial resolution of 30×30

m for six of its bands, and the Landsat MSS has a nominal spatial resolution of 79 x 79 m. Generally, the smaller the spatial resolution, the greater the resolving power of the sensor system. Figure 1-8 depicts digital camera imagery of an area in Mechanicsville, N.Y. at resolutions ranging from 0.5 x 0.5 m to 80 x 80 m. Note that there is not a significant difference in the interpretability of 0.5 x 0.5 m data, 1 x 1 m data, and even 2 x 2 m data. However, the urban information content decreases rapidly when using 5 x 5 m imagery and is practically useless for urban analysis at spatial resolutions larger than 10 x 10 m. Landsat MSS data is particularly useless (79 x 79 m) for most urban applications.

Another useful rule is that in order to detect a feature, the spatial resolution of the sensor system should be less than one-half the size of the feature measured in its smallest dimension. For example, if we want to identify the location of all oak trees within a city park, the minimum acceptable spatial resolution would be approximately one-half the diameter of the smallest oak tree crown. Even this spatial resolution, however, will not guarantee success if there is no difference between the spectral response of the oak tree (the object) and the soil or grass surrounding it (i.e., its background).

Temporal Resolution: The *temporal resolution* of a remote sensing system refers to how often it records imagery of a particular area. For example, the temporal resolution of the sensor system shown in Figure 1-9a is every 16 days. Ideally, the sensor obtains data repetitively to capture unique discriminating characteristics of the object under investigation (Haack et al., 1997). For example, agricultural crops have unique crop calendars in each geographic region. To measure specific agricultural variables, it is necessary to acquire remotely sensed data at critical dates in the phenological cycle. Analysis of multiple-date imagery provides information on how the variables are changing through time. Change information provides insight into processes influencing the development of the crop (Steven, 1993). Fortunately, several satellite sensor systems such as SPOT are pointable, meaning that they can acquire imagery off-nadir (*nadir* is the point directly beneath the spacecraft) if necessary. This dramatically increases the probability that imagery might be obtained during a growing season or during an emergency. However, the off-nadir oblique viewing also introduces bidirectional reflectance distribution function (BRDF) issues that are addressed in Chapter 10 (Remote Sensing of Vegetation).

Radiometric Resolution: This is defined as the sensitivity of a remote sensing detector to differences in signal strength as it records the radiant flux reflected or emitted from the terrain. It defines the number of just discriminable signal levels; consequently, it can have a significant impact on our ability to measure the properties of scene objects. For example, the original multispectral scanner (MSS) onboard Landsat 1 recorded the reflected radiant energy with a precision of 6-bits (values ranging from 0 to 63). Landsat 4 and 5 Thematic Mapper recorded data in 8-bits (values from 0 to 255). Thus, the Landsat TM sensor had improved radiometric resolution when compared with the original MSS. Several new sensor systems have 12-bit radiometric resolution (values ranging from 0 to 4095) (Figure 1-9b).

Improvements in resolution generally increase the probability that phenomena may be remotely sensed more accurately. The trade-off is that any improvement in resolution will usually require additional data-processing capability for either human or computer-assisted analysis.

Suborbital (Airborne) Remote Sensing Systems

High-quality metric cameras mounted onboard aircraft continue to provide aerial photography for many Earth resource applications. For example, the U.S. Geological Survey's National Aerial Photography Program (NAPP) systematically collects 1:40,000-scale black-and-white or color-infrared aerial photography of much of the United States every 5 to 10 years. In addition, sophisticated remote sensing systems are routinely mounted on aircraft to provide high spatial and spectral resolution multispectral remotely sensed data. Examples include the Compact Airborne Spectrographic Imager (CASI), Daedalus multispectral scanners, and NASA's Airborne Terrestrial Applications Sensor (ATLAS) (Table 1-3). These sensors can collect data on demand when disaster strikes (e.g., oil spills or floods) if cloud-cover conditions permit. There are also numerous radars, such as Intermap's Star-3i radar, that can be flown on aircraft day and night and in inclement weather. Unfortunately, suborbital remote sensor data are usually expensive to acquire per km^2. Also, atmospheric turbulence can cause the data to have severe geometric distortions that can be quite difficult to correct.

Current and Proposed Satellite Remote Sensing Systems

Remote sensing systems onboard satellites provide high-quality, relatively inexpensive data per km^2. For example, the European Remote Sensing Satellite (ERS-1,2) collects 26 × 28 m spatial resolution C-band active microwave (radar) imagery of much of Earth, even through clouds. Similarly, the Canadian Space Agency RADARSAT obtains C-band active microwave imagery. The United States has pro-

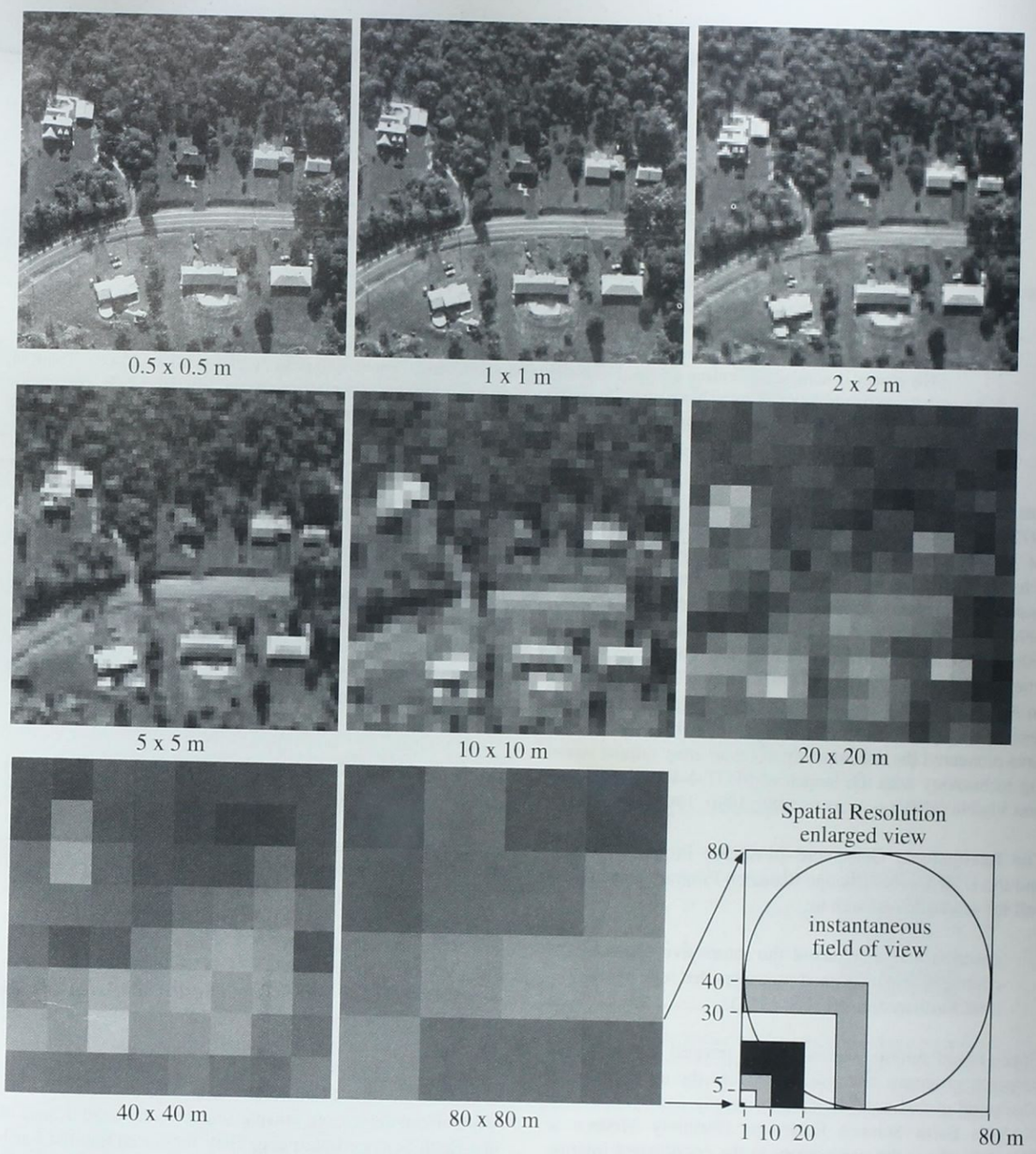

Figure 1-8 Imagery of residential housing near Mechanicsville, NY. The data were obtained on June 1, 1998, at a nominal spatial resolution of 0.3 x 0.3 m (approximately 1 x 1 ft) using a digital camera (courtesy of Litton Emerge, Inc.). The original data were resampled to derive the imagery with the simulated spatial resolutions shown.

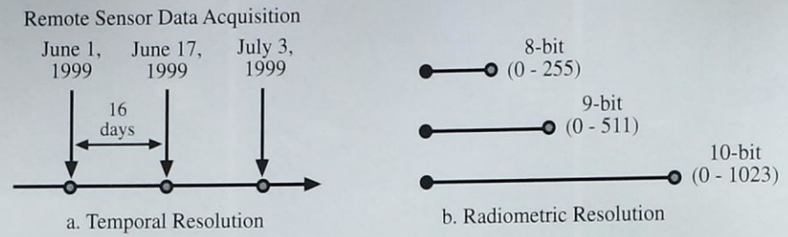

Figure 1-9 a) The temporal resolution of a remote sensing system refers to how often it records imagery of a particular area. This example depicts the systematic collection of data every 16 days, presumably at approximately the same time of day. Landsat Thematic Mapper 4 and 5 had 16-day revisit cycles. b) The radiometric resolution of a remote sensing system is defined as the sensitivity of remote sensing detectors to differences in signal strength as it records the radiant flux reflected or emitted from the terrain. The energy is normally quantized during the analog-to-digital (A-to-D) conversion process to 8, 9, 10, or 12-bits. Think of radiometric resolution as being like a ruler. If you had to measure something very precisely, would you rather have a ruler with just 256 subdivisions (8-bit) or one with 1024 subdivisions (10-bit)? Several new sensor systems record data in 12-bits (0-4095).

gressed from multispectral scanning systems (Landsat MSS, 1972 to present) to more advanced scanning systems (Landsat Thematic Mapper, 1982 to present). The Land Remote Sensing Policy Act of 1992 specified the future of satellite land remote sensing programs in the United States (Asker, 1992; Jensen, 1992). Unfortunately, Landsat 6, with its Enhanced Thematic Mapper (ETM), did not achieve orbit when launched on October 5, 1993. Landsat 7 was launched on April 15, 1999, to relieve the United States' land remote sensing data gap (Henderson, 1994). Meanwhile, the French have pioneered the development of linear array remote sensing technology with the launch of SPOT 1-4 High Resolution Visible (HRV) sensors in 1986, 1990, 1993, and 1998.

The International Geosphere–Biosphere Program (IGBP) and the U. S. Global Change Research Program (USGCRP) call for scientific research to:

> describe and understand the interactive physical, chemical, and biological processes that regulate the total Earth system (CEES, 1991).

Space-based remote sensing is an integral part of these research programs because it provides the only means of observing global ecosystems consistently and synoptically. NASA's Earth Science Enterprise (formerly Mission to Planet Earth) is the name given to the coordinated international plan to provide the necessary satellite platforms and instruments, an Earth Observing System Data and Information System (EOSDIS), and related scientific research for IGBP. In particular, new satellite remote sensing instruments will include 1) a series of near-term Earth probes to address discipline-specific measurement needs, 2) a series of multi-purpose polar orbiting platforms, initiated in 1988, to acquire 15 years of continuous Earth observations, called the Earth Observing System (EOS), and 3) a series of geostationary platforms carrying advanced multidisciplinary instruments to fly sometime after the year 2000, called the Geostationary Earth Observing System (Price et al., 1994; NASA, 1998). Not everyone is convinced that NASA's Earth Science Enterprise is the most economic way of obtaining the required environmental information (e.g., Hudgins, 1997).

The first of the National Aeronautics and Space Administration Mission to Planet Earth sensors placed in orbit was the Upper Atmosphere Research Satellite (UARS) launched in 1991 (Luther, 1992). The UARS sensors collected information on upper atmospheric chemistry, temperature, wind speed, direction, and energy inputs. The TOPEX/POSEIDON satellite launched in 1992 uses radar altimetry to measure sea-surface height over 90 percent of the world's ice-free oceans. The system acquires global maps of ocean topography (barely perceptible hills and valleys of the sea surface), which scientists use to calculate the speed and direction of ocean currents (Jones, 1992).

The EOS Science Plan: Asrar and Dozier (1994) conceptualized the remote sensing science conducted as part of the Earth Science Enterprise. They suggested that the Earth consists of two subsystems, 1) the physical climate, and 2) biogeochemical cycles, linked by the global hydrologic cycle, as shown in Figure 1-10.

The *physical climate* subsystem is sensitive to fluctuations in the Earth's radiation balance. Human activities have caused

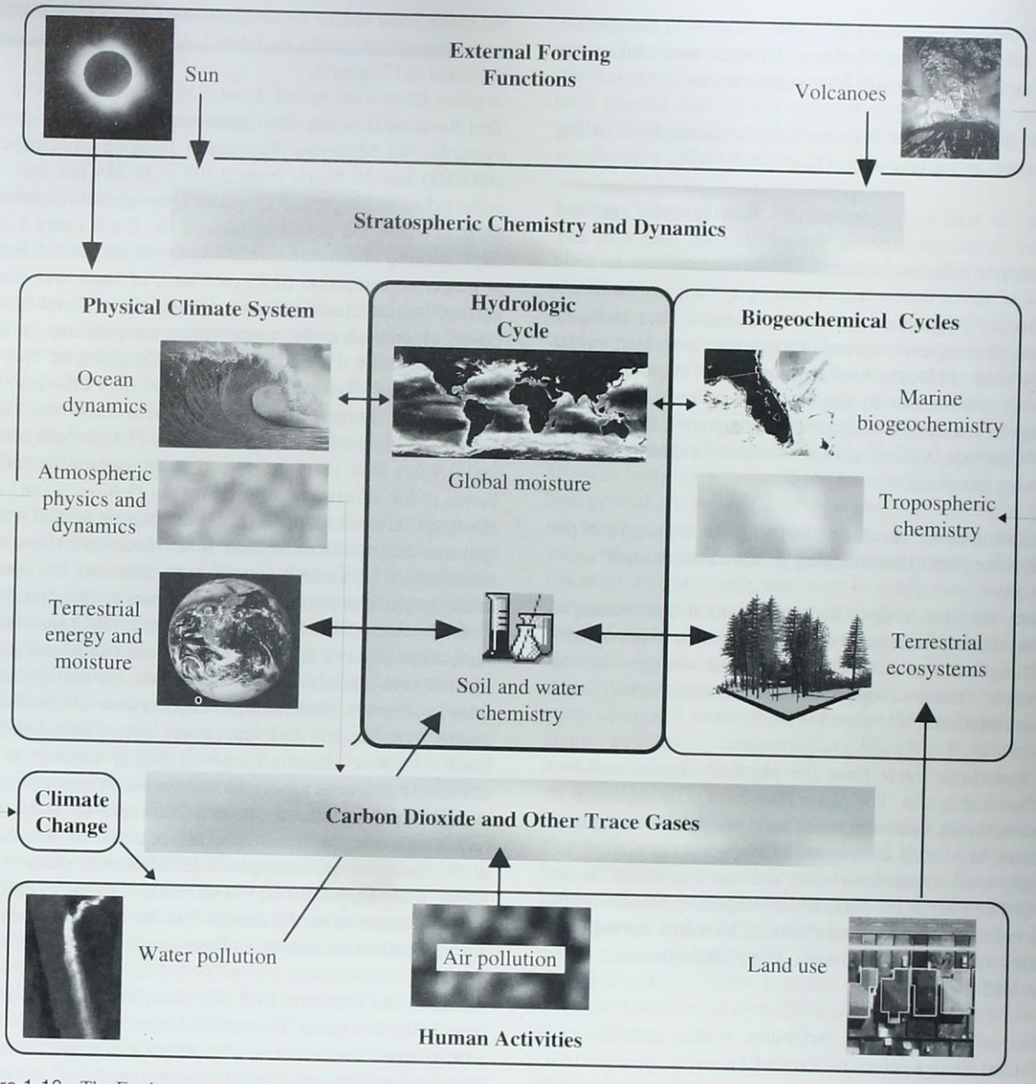

Figure 1-10 The Earth system may be subdivided into two subsystems — the physical climate system and biogeochemical cycles — that are linked by the global hydrologic cycle. Significant changes in the external forcing functions and human activities can have a dramatic impact on the physical climate system, biogeochemical cycles, and the global hydrologic cycle. Examination of these subsystems and their linkages defines the critical questions that the NASA Earth Observing System (EOS) is attempting to answer (after Asrar and Dozier, 1994).

changes to the planet's radiative heating mechanism that rival or exceed natural change. For example, increases in greenhouse gases between 1765 and 1990 have caused a radiative forcing of 2.5 W m^{-2}. If this rate is sustained, it could result in global mean temperatures increasing about 0.2 to 0.5˚C per decade during the next century. Volcanic eruptions and the ocean's ability to absorb heat may impact the projections. Nevertheless, the following important questions are being addressed using remote sensing (Asrar and Dozier, 1994):

- How do clouds, water vapor, and aerosols in the Earth's radiation and heat budgets change with increased atmospheric greenhouse-gas concentrations?

- How do the oceans interact with the atmosphere in the transport and uptake of heat?

- How do land-surface properties such as snow and ice cover, evapotranspiration, urban/suburban land use, and vegetation influence circulation?

The Earth's *biogeochemical cycles* have also been changed by man. Atmospheric carbon dioxide has increased by 30 percent since 1859, methane by more than 100 percent, and ozone concentrations in the stratosphere have decreased, causing increased levels of ultraviolet radiation to reach the Earth's surface. Global change research is addressing the following questions:

- What role do the oceanic and terrestrial components of the biosphere play in the changing global carbon budget?

- What are the likely effects on natural and managed ecosystems of increased carbon dioxide, acid deposition, shifting patterns of precipitation, and changes in soil erosion, river chemistry, and atmospheric ozone concentrations?

The *hydrologic cycle* links the physical climate and biogeochemical cycles. The phase change of water between its gaseous, liquid, and solid states involves storage and release of latent heat, so it influences atmospheric circulation and globally redistributes both water and heat (Asrar and Dozier, 1994). The hydrologic cycle is the integrating process for the fluxes of water, energy, and chemical elements among components of the Earth System. Important questions to be addressed include:

- How will atmospheric variability, human activities, and climate change affect patterns of humidity, precipitation, evapotranspiration, and soil moisture?

- How does soil moisture vary in time and space?

- Can we predict changes in the global hydrologic cycle using present and future observation systems and models?

EOS AM-1 (now referred to as the *Terra* satellite) houses five remote sensing instruments designed to address many of the previously mentioned research topics (NASA, 1998). The spatial, spectral, and temporal characteristics of three of the main *Terra* sensor systems (*MODIS*, *ASTER*, and *MISR*) are summarized briefly in Table 1-3, with additional detail provided in Chapter 7.

The *Terra* sensors use new remote sensing technology. For example, the Moderate Resolution Imaging Spectrometer (*MODIS*) has 36 bands from 0.405 – 14.385 μm that will collect data at 250- and 500-m and 1-km spatial resolutions. *MODIS* views the entire surface of the Earth every 1 to 2 days, making observations in 36 coregistered spectral bands, at moderate resolution (0.25 to 1 km), of land- and ocean-surface temperature, primary productivity, land-surface cover, clouds, aerosols, water vapor, temperature profiles, and fires (NASA, 1998). The Advanced Spaceborne Thermal Emission and Reflection Radiometer (*ASTER*) has five bands in the thermal infrared region between 8 and 12 μm with 90-m pixels. It also has three broad bands between 0.5 and 0.9 μm with 15-m pixels and stereo capability, and six bands in the shortwave infrared region (1.6 – 2.5 μm) with 30-m spatial resolution. *ASTER* is the highest spatial resolution sensor system on the EOS *Terra* platform and provides information on surface temperature that can be used to model evapotranspiration. The Multi-angle Imaging SpectroRadiometer (*MISR*) has nine separate CCD pushbroom cameras to observe Earth in four spectral bands and at nine separate view angles. It provides data on clouds, atmospheric aerosols, and multiple-angle views of the Earth's deserts, vegetation, and ice cover. The Clouds and the Earth's Radiant Energy System (*CERES*) consists of two scanning radiometers that measure the Earth's radiation balance and provide cloud property estimates to assess their role in radiative fluxes from the surface of the earth to the top of the atmosphere. Finally, *MOPITT* (Measurements of Pollution in the Troposphere) is a scanning radiometer that provides information on the distribution, transport, sources, and sinks of carbon monoxide and methane in the troposphere.

Commercial Vendors: EOSAT, Inc., launched Landsat 6 with its Enhanced Thematic Mapper in 1993. Unfortunately, it failed to achieve orbit. EarthWatch, Inc. launched Earlybird in December, 1997. Unfortunately, all communication with the satellite was lost. Space Imaging, Inc. launched IKONOS on April 27, 1999 and it failed to achieve orbit. A second IKONOS satellite was launched on September 24, 1999. The IKONOS sensor system has a 1 x 1 m panchromatic band as well as four 4 x 4 m multispectral bands (Table 1-3). Similar sensor systems are scheduled to be launched by EarthWatch, Inc. (*Quickbird*) and ORBIMAGE, Inc. (*Orbview 3*) in 2000. ORBIMAGE also plans to launch a hyperspectral satellite remote sensing system in 2000 (*Orbview 4*).

Remote Sensing Data Analysis

The analysis of remotely sensed data is performed using a variety of image processing techniques (Figure 1-11), including:

- analog (visual) image processing of image data and

- digital image processing of digital data.

Both analog and digital image processing should allow the analyst to perform *scientific visualization,* defined as "visually exploring data and information in such a way as to gain understanding and insight into the data" (Pickover, 1991). First, however, it is instructive to ask two questions: Why process the remotely sensed data digitally at all? Isn't visual image analysis sufficient?

Human beings are exceptionally adept at visually interpreting images produced by certain types of remote sensing devices, especially cameras. We could ask, Why try to mimic or improve on this capability? First, there are certain thresholds beyond which the human interpreter cannot detect "just noticeable differences" in the imagery. For example, it is commonly known that an analyst can discriminate only about nine shades of gray when interpreting continuous-tone black-and-white aerial photography. If the data were originally recorded with 256 shades of gray, there may be more subtle information present in the image than the interpreter can extract visually. Furthermore, the interpreter brings to the task all the pressures of the day, making the interpretation generally unrepeatable. Conversely, the results obtained by computer are repeatable (even when wrong!). Also, when it comes to keeping track of a great amount of detailed quantitative information, such as the spectral characteristics of a vegetated field throughout a growing season for crop identification purposes, the computer is very adept at storing and manipulating such tedious information and possibly making a more definitive conclusion as to what crop is being grown. This is not to say that digital image processing is superior to visual image analysis. This is certainly not the case. Rather, there may be times when a digital approach is better suited to the problem at hand.

But what about the actual processes of analog (visual) versus digital image processing? Are there similarities between the goals and methods of both procedures? Estes et al. (1983) suggest that there exist several image-analysis tasks and basic elements of image interpretation that the visual and digital image processing approaches share (Figure 1-11). First, both manual and digital analysis of remotely sensed data seek to detect and identify important phenomena in the scene. Once identified, the phenomena are usually measured, and the information is used in problem solving. Thus, both manual and digital analysis have the same general goals. However, the attainment of these goals may follow significantly different paths.

Analog (Visual) Image Processing

Most of the fundamental elements of image interpretation identified in Figure 1-11 are used in visual image analysis, including size, shape, shadow, color (tone), parallax, pattern, texture, site, and association. The human mind is amazingly adept at recognizing these complex elements in an image or photograph because we constantly process profile views of Earth features every day and continually process images in books and magazines and on television. Furthermore, we are adept at bringing to bear all the knowledge in our personal background and collateral information. We then converge all this evidence to identify phenomena in images and/or to judge their significance. Precise measurement of objects (location, height, width, etc.) may be performed using optical photogrammetric techniques applied to either monoscopic (single-photo) or stereoscopic (overlapping) images. Numerous books have been written on how to perform visual image interpretation and photogrammetric measurement. Chapter 5 summarizes the use of the fundamental elements of image interpretation. Chapter 6 introduces photogrammetry principles.

Interestingly, there is a resurgence in the art and science of visual photointerpretation as the digital remote sensor systems provide higher spatial resolution imagery. For example, Indian IRS-1C panchromatic data (5.8 × 5.8 m) is often photointerpreted and used as a base map in GIS projects. The new 1 x 1 m panchromatic data provided by commercial companies (e.g., Space Imaging IKONOS, ORBIMAGE Orbview 3) will cause even more visual image interpretation to take place.

Digital Image Processing

Scientists have made significant advances in digital image processing of remotely sensed data for scientific visualization and hypothesis testing. The methods are summarized in the companion book by Jensen (1996) and others (e.g., Wolff and Yaeger, 1993; Nadler and Smith, 1993; Schott, 1997). The major types of digital image processing include statistical and syntactical pattern recognition, photogrammetric image processing of stereoscopic imagery, hyperspectral data analysis, and expert system and neural network image analysis.

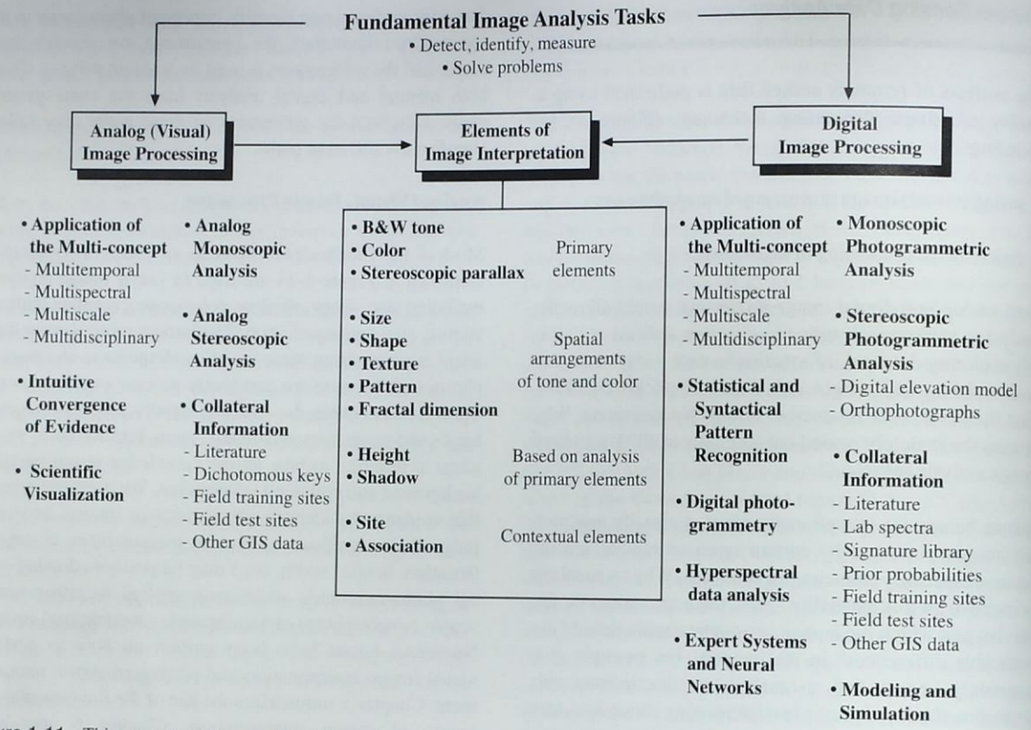

Figure 1-11 This conceptual diagram identifies analog (visual) and computer-assisted digital image processing of remotely sensed data that rely on the analysis of the fundamental elements of image interpretation. Visual analysis at the present time incorporates many more of the complex elements in the analysis of remote sensing images.

Pattern Recognition: Fundamental statistical methods of rectifying remotely sensed data to a map projection, enhancing the data, classifying the data into land use and land cover, and identifying change between dates of imagery are now performed routinely with reasonable precision. Interestingly, most of the computer-assisted image processing to date has involved the use of only a few of the basic elements of image interpretation. In fact, the overwhelming majority of all digital image analysis appears to be dependent primarily on just the *tone* or *color* of individual pixels in the scene using fundamental statistical pattern recognition techniques (Figure 1-11).

Various techniques have been used to incorporate additional elements of image interpretation into the image analysis process. For example, numerous studies have synthesized *texture* information from the spectral data in the imagery. Some have computed the fractal dimension of images and found it to be a valuable element of image interpretation (Emerson et al., 1999). *Contextual* classification has been performed, which makes use of neighboring pixel values, thus incorporating some level of *association* information (Gong and Howarth, 1992). Some image processing now takes into account *fuzzy set logic*, which attempts to model the imprecision in the real world (Ji and Jensen, 1996).

Photogrammetry: Significant advances have been made in the analysis of stereoscopic remote sensor data using computer workstations and digital image processing photogrammetric algorithms (Li, 1998). Soft-copy photogrammetric workstations can be used to extract accurate digital elevation models (DEMs) and differentially corrected orthophotography from the triangulated aerial photography or imagery (Ackerman, 1994; Jensen, 1995). The technology is revolutionizing the way DEMs are collected, especially for developing countries and how orthophotos are produced for rural and urban-suburban applications.

Hyperspectral: Analysts should be aware that special software is required to process the hyperspectral data from spectroradiometer remote sensor systems (e.g., AVIRIS, *MODIS*). Kruse et al. (1992), Landgrebe (1999) and ENVI (1999) have pioneered the development of hyperspectral image analysis software. The software reduces the dimensionality of the data (number of bands) to a manageable degree, while still retaining the essence of the data. Under certain conditions the software can be used to compare the remotely sensed spectral reflectance curves with a library of spectral reflectance curves. Analysts are also able to identify the type and proportion of different materials within an individual picture element (referred to as end-member analysis). This is an exciting area of digital image processing.

Expert Systems and Neural Networks: Humans are very successful at visually interpreting aerial photographs because they focus their real-world knowledge about the study area and their years of visual processing experience on the task. It is difficult to make a computer understand and use the heuristic rules of thumb and knowledge that a human expert uses when interpreting an image (Moller-Jensen, 1990). Nevertheless, there has been considerable success in the use of artificial intelligence (AI) to try to make computers do things that, at the moment, people do better. One area of AI that has great potential in remote sensing image analysis is the use of expert systems. Expert systems can be used to 1) interpret an image, and/or 2) place all the information contained within an image in its proper context with other ancillary data and extract more valuable information (Bolstad and Lillesand, 1992). In the first case, collateral data and rules specified by an expert might be used by novices to more accurately interpret a remotely sensed image (Huang and Jensen, 1998). In the second case, an expert system might be used to produce geological engineering maps from input datasets (bedrock geology, agricultural soils, topography), some of which were derived using remote sensing (Usery et al., 1988). Scientists with good training in an Earth science discipline, an understanding of remote sensing, and expert system skills (e.g., how to create a knowledge base and query it with an inference engine) will make significant contributions in this area.

Neural networks have also been used to analyze remotely sensed data (Hepner et al., 1990; Jensen and Qiu, 1999). Neural networks do not require the input data to be normally distributed. Furthermore, they can be programmed to learn.

Modeling Remote Sensing Data Using A GIS Approach

Remotely sensed data should not be analyzed in a vacuum without the benefit of other collateral information, such as soils, hydrology, and topography (Price et al., 1994; Ramsey et al., 1995). Unfortunately, many scientists promoting the integration of remote sensing and GIS assume that the flow of data should be unidirectional — that is, from the remote sensing system to the GIS. Actually, the backward flow of ancillary data from the GIS to the remote sensing system is very valuable (Stow, 1993). For example, land-cover mapping using remotely sensed data has been significantly improved by incorporating topographic information from digital terrain models and other GIS data (Franklin and Wilson, 1992). Basically, the interface between GIS and remote sensing systems is functional but weak (Lunetta et al., 1991). Each technology suffers from a lack of critical support that could be provided by the other. GIS needs timely, accurate updating of the spatially distributed variables in the database that remote sensing can provide. Remote sensing can benefit from access to accurate ancillary information to improve classification accuracy and other types of modeling (Jensen et al., 1994). Such synergy is critical if successful expert system and neural network analyses are to be performed.

Scene Modeling

Strahler et al. (1986) describe a framework for modeling in remote sensing. Basically, a remote sensing model has three components: 1) a scene model, which specifies the form and nature of the energy and matter within the scene and their spatial and temporal order; 2) an atmospheric model, which describes the interaction between the atmosphere and the energy entering and being emitted from the scene; and 3) a sensor model, which describes the behavior of the sensor in responding to the energy fluxes incident on it and in producing the measurements that constitute the image. They suggest that "the problem of scene inference, then, becomes a problem of model inversion in which the order in the scene is reconstructed from the image and the remote sensing model." For example, Li and Strahler (1985) modeled the optical-geometric properties of a coniferous forest canopy that has been tested extensively (Franklin and Turner, 1992; Woodcock et al., 1997).

Basically, successful remote sensing modeling predicts how much radiant flux in certain wavelengths should exit a particular object (e.g., a conifer canopy) even without actually sensing the object. When the model's prediction is the same as the sensor's measurement, the relationship has been modeled correctly. The scientist then has a greater appreciation for energy-matter interactions in the scene and may be able to extend the logic to other regions or applications with confidence. The remote sensor data can then be used more effectively in physical deterministic models (e.g., watershed runoff, net primary productivity, and evapotranspiration models), which are so important for large ecosystem modeling. Recent work allows one to model the utility of sensors

with different spatial resolutions for particular applications such as urban analysis (Collins and Woodcock, 1999).

Information Presentation

Information derived from remote sensor data are usually summarized as an enhanced image, image map, orthophotomap, thematic map, spatial database file, statistic, or graph (Figure 1-5). Thus, the final output products often require knowledge of remote sensing, cartography, GIS, and spatial statistics as well as the systematic science being investigated (e.g., soils, agriculture, forestry, wetland, urban studies). Scientists who understand the rules and synergistic relationship between the technologies can produce output products that communicate effectively. Conversely, those who violate fundamental rules (e.g., cartographic theory or database topology design) often produce poor output products that do not communicate effectively.

Image maps offer scientists an alternative to line maps for many cartographic applications. Thousands of satellite image maps have been produced from Landsat MSS (1:250,000 and 1:500,000 scale), TM (1:100,000 scale) and AVHRR data (Vickers, 1993). Image maps at scales of >1:24,000 are possible with the improved resolution of 1 x 1 m data (Li, 1998). Because image map products can be produced for a fraction of the cost of conventional line maps, they provide the basis for a national map series oriented toward the exploration and economic development of the less developed areas of the world, most of which have not been mapped at scales of 1:100,000 or larger.

Remote sensor data that has been geometrically rectified to a standard map projection is becoming indispensable in most sophisticated GIS databases. This is especially true of orthophotomaps that have the metric qualities of a line map and the information content of an aerial photograph or other type of image (Jensen, 1995).

Unfortunately, *error* is introduced at various stages in the remote sensing process and must be identified and reported. Innovations in error reduction include: 1) recording the genealogy or lineage of the various operations applied to the original remote sensor data (Lanter and Veregin, 1992), 2) documenting the geometric (spatial) error and thematic (attribute) error of the individual source materials, 3) improving legend design, especially for change detection map products derived from remote sensing, and 4) precise error evaluation statistic reporting (Khorram et al., 1999). Many of these concerns have not been adequately addressed. The remote sensing and GIS community should incorporate technologies that carefully track all types of error entering final map and image products (Goodchild and Gopal, 1992). This will result in more accurate information being used in the decision-making process.

Earth Resource Analysis Perspective

Remote sensing may be used for numerous applications, including weapon guidance systems (e.g., the cruise missile), medical image analysis (e.g., X-raying a broken arm), nondestructive evaluation of machinery and products (e.g., on an assembly line), and analysis of Earth's resources. Earth resource information is defined as any information concerning terrestrial vegetation, soils, minerals, rocks, water, and urban infrastructure as well as certain atmospheric characteristics. *This book focuses on the art and science of applying remote sensing for the extraction of useful Earth resource information.* Such information may be useful for modeling the global carbon cycle, the biology and biochemistry of ecosystems, aspects of the global water and energy cycle, climate variability and prediction, atmospheric chemistry, characteristics of the solid Earth, and natural hazards (Paylor et al., 1999).

Book Organization

This chapter defined important terms and provided a perspective on how remote sensing science can be useful for Earth resource investigations. Chapter 2 introduces the fundamental principles of electromagnetic radiation and how this radiation is used to perform remote sensing of the environment. Chapter 3 reviews the history of photography, and aerial and satellite platforms. Chapter 4 introduces the fundamental characteristics of aerial photography, filtration, and film. Chapter 5 presents the fundamental elements of visual image interpretation. Chapter 6 reviews principles of photogrammetry used to extract quantitative information from aerial photography. Chapter 7 presents the characteristics of optical-mechanical remote sensing systems. Chapter 8 introduces thermal infrared remote sensing. Chapter 9 presents active microwave remote sensing. Chapter 10 reviews how remote sensing may be used to extract fundamental biophysical characteristics of terrestrial and aquatic vegetation. Chapter 11 provides insight into remote sensing of terrestrial water, ice, and snow as well as atmospheric water vapor and temperature. Chapter 12 demonstrates how remote sensing can provide unique urban/suburban infrastructure information using a variety of remote sensing systems. Chapter 13 describes how selected soil and mineral characteristics may be remotely sensed and how major geomorphic features on the surface of the Earth may be identified.

References

Ackerman, F., 1994, "Digital Elevation Models: Techniques and Application, Quality Standards, Development," *Proceedings,* Symposium on Mapping and Geographic Information Systems, Athens, GA: International Society for Photogrammetry & Remote Sensing, 30(4):421–432.

American Society of Photogrammetry, 1944, 1952, 1966, *Manual of Photogrammetry,* Falls Church: ASP, multiple editions.

Asker, J. R., 1992, "Congress Considers Landsat 'Decommercialization' Move," *Aviation Week and Space Technology,* May 11, 18–19.

Asrar, G. and J. Dozier, 1994, *EOS: Science Strategy for the Earth Observing System,* Woodbury: American Institute of Physics.

Bolstad, P. V. and T. M. Lillesand, 1992, "Rule-based Classification Models: Flexible Integration of Satellite Imagery and Thematic Spatial Data," *Photogrammetric Engineering & Remote Sensing,* 58(7):965–971.

Budge, A. and S. A. Morain, 1995, "Access Remote Sensing Data for GIS," *GIS World,* 8(2):45–49.

Canadian Space Agency, 1999, *RADARSAT,* Saint-Hubert: RADARSAT Program.

CEES, 1991, *Our Changing Planet: The FY 1992 U.S. Global Change Research Program,* Committee on Earth and Environmental Sciences, Office of Science & Technology, Washington, DC, 21 pp.

Clark, R. N., 1999, *Spectroscopy of Rocks and Minerals, and Principles of Spectroscopy,* Denver: U.S. Geological Survey, http://speclab.cr.usgs.gov, 58 pp.

Collins, J. B. and C. E. Woodcock, 1999, "Geostatistical Estimation of Resolution-Dependent Variance in Remotely Sensed Images," *Photogrammetric Engineering and Remote Sensing,* 65(1):41–50.

Colwell, R. N. (Ed.), 1960, *Manual of Photographic Interpretation,* Falls Church, VA: American Society for Photogrammetry & Remote Sensing.

Colwell, R. N. (Ed.), 1983, *Manual of Remote Sensing,* 2nd. Ed., Falls Church, VA: American Society of Photogrammetry.

Colwell, R. N., 1984, "From Photographic Interpretation to Remote Sensing," *Photogrammetric Engineering and Remote Sensing,* 50(9):1305.

Colwell, R. N., 1997, "History and Place of Photographic Interpretation," *Manual of Photographic Interpretation,* W. R. Philipson (Ed.), 2nd Ed., Bethesda: American Society for Photogrammetry & Remote Sensing, 33–48.

Congalton, R. G. and K. Green, 1998, *Assessing the Accuracy of Remotely Sensed Data,* Boca Raton: Lewis, 137 pp.

Cracknell, A. P. and L. W. B. Hayes, 1993, *Introduction to Remote Sensing,* London: Taylor & Francis, 293 pp.

Curran, P. J., 1987, "Remote Sensing Methodologies and Geography," *International Journal of Remote Sensing,* 8:1255–1275.

Dahlberg, R. W. and J. R. Jensen, 1986, "Education for Cartography and Remote Sensing in the Service of an Information Society: The United States Case," *The American Cartographer,* 13(1):51–71.

Davis, B. A., 1999, "An Overview of NASA's Commercial Remote Sensing Program," *Earth Observation Magazine,* 8(3):58–60.

Dobson, J. E., 1993, "Commentary: A Conceptual Framework for Integrating Remote Sensing, Geographic Information Systems, and Geography," *Photogrammetric Engineering & Remote Sensing,* 59(10):1491–1496.

Duggin, M. J. and C. J. Robinove, 1990, "Assumptions Implicit in Remote Sensing Data Acquisition and Analysis," *International Journal of Remote Sensing,* 11(10):1669–1694.

Eidenshink, J. C., 1992, "1990 Conterminous United States AVHRR Data Set," *Photogrammetric Engineering & Remote Sensing,* 58(6):809–813.

Emerson, C. W., N. Lam, and D. A. Quattrochi, 1999, "Multi-scale Fractal Analysis of Image Texture and Pattern," *Photogrammetric Engineering & Remote Sensing,* 65(1):51–61.

Engman, E. T. and N. Chauhan, 1995, "Status of Microwave Soil Moisture Measurements with Remote Sensing," *Remote Sensing of Environment,* 51:189–198.

ENVI, 1999, *ENVI User's Guide: Environment for Visualizing Images,* Boulder: Research Systems, Inc., 500 pp.

Ramsey, R. D., A. Falconer and J. R. Jensen, 1995, "The Relationship Between NOAA-AVHRR Normalized Difference Vegetation Index and Ecoregions in Utah," *Remote Sensing of Environment*, 53:188–198.

Rivard, B. and R. E. Arvidson, 1992, "Utility of Imaging Spectrometry for Lithologic Mapping in Greenland," *Photogrammetric Engineering & Remote Sensing*, 58(7):945–949.

Robbins, J., 1999, "High-Tech Camera Sees What Eye Cannot," *New York Times*, Science Section, September 14, D5.

Ryerson, R., 1989, "Image Interpretation Concerns for the 1990s and Lessons from the Past," *Photogrammetric Engineering & Remote Sensing*, 55(10):1427–1430.

Schott, J. R., 1997, *Remote Sensing —the Image Chain Approach*, New York: Oxford University Press, 394 pp.

Steven, M. D., 1993, "Satellite Remote Sensing for Agricultural Management: Opportunities and Logistic Constraints," *ISPRS Journal of Photogrammetry & Remote Sensing*, 48(4):29–34.

Stow, D. A., 1993, "The Role of GIS for Landscape Ecological Studies," *Landscape Ecology and GIS*, R. Haines-Young, D. Green, and S. Cousins, Eds., NY: Taylor & Francis, 11–21.

Strahler, A. H., C. E. Woodcock and J. A. Smith, 1986, "On the Nature of Models in Remote Sensing," *Remote Sensing of Environment*, 20:121–139.

Usery, E. L., P. Altheide, R. R. Deister and D. J. Barr, 1988, "Knowledge-based Geographic Information System Techniques Applied to Geological Engineering," *Photogrammetric Engineering & Remote Sensing*, 54(11):1623–1628.

Vickers, E. W., 1993, "Production Procedures for an Oversize Satellite Image Map," *Photogrammetric Engineering & Remote Sensing*, 59(2):247–254.

Walsh, S. J., T. P. Evans, W. F. Welsh, B. Entwisle and R. R. Rindfuss, 1999, "Scale-dependent Relationships Between Population and Environment in Northeastern Thailand," *Photogrammetric Engineering & Remote Sensing*, 65(1):97–105.

Wolff, R. S. and L. Yaeger, 1993, *Visualization of Natural Phenomena*, Santa Clara, CA: Telos Springer-Verlag, 374 pp.

Wolter, J. A., 1975, *The Emerging Discipline of Cartography*, Minneapolis: University of Minnesota, Department of Geography, unpublished dissertation.

Woodcock, C. E., J. B. Collins, V. Jakabhazy, X. Li, S. Macomber and Y. Wu, 1997, "Inversion of the Li-Strahler Canopy Reflectance Model for Mapping Forest Structure," *IEEE Transactions on Geoscience and Remote Sensing*, 35(2):405–414.

Wright, D. J., M. F. Goodchild and J. D. Procter, 1997, "GIS: Tool or Science; Demystifying the Persistent Ambiguity of GIS as Tool versus Science," *The Professional Geographer*, 87(2):346–362.

Electromagnetic Radiation Principles 2

Energy recorded by remote sensing systems undergoes fundamental interactions that should be understood to properly interpret the remotely sensed data. For example, if the energy being remotely sensed comes from the Sun, the energy

- is radiated by atomic particles at the source (the Sun),
- propagates through the vacuum of space at the speed of light,
- interacts with the Earth's atmosphere,
- interacts with the Earth's surface,
- interacts with the Earth's atmosphere once again, and
- finally reaches the remote sensor, where it interacts with various optical systems, filters, film emulsions, or detectors.

It is instructive to examine each of these fundamental interactions that electromagnetic energy undergoes as it progresses from its source to the remote sensing system detector.

Conduction, Convection, and Radiation

Energy is the ability to do work. In the process of doing work, energy is often transferred from one body to another or from one place to another. The three basic ways in which energy can be transferred include conduction, convection, and radiation (Figure 2-1). Most people are familiar with *conduction* that occurs when one body (molecule or atom) transfers its kinetic energy to another by colliding with it. This is how a metal pan is heated by a hot burner on a stove. In *convection*, the kinetic energy of bodies is transferred from one place to another by physically moving the bodies. A good example is the heating of the air near the ground in the morning hours. The warmer air near the surface rises, setting up convectional currents in the atmosphere, which may produce cumulus clouds. The transfer of energy by electromagnetic *radiation* is of primary interest to remote sensing science because it is the only form of energy transfer that can take place in a vacuum such as the region between the Sun and the Earth.

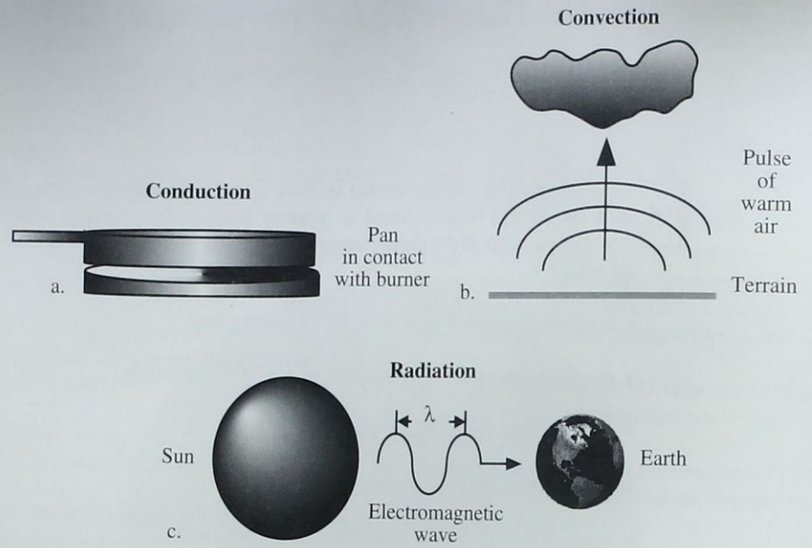

Figure 2-1 Heat may be transferred in three ways: conduction, convection, and radiation. a) Heat may be conducted directly from one object to another as when a pan is in direct physical contact with a hot burner. b) The Sun bathes the Earth's surface with radiant energy causing the air near the ground to increase in temperature. The less dense air rises creating convectional currents in the atmosphere. c) Electromagnetic energy in the form of electromagnetic waves may be transmitted through the vacuum of space from the Sun to the Earth.

Electromagnetic Radiation Models

To understand how electromagnetic radiation is created, how it propagates through space, and how it interacts with other matter, it is useful to describe the processes using two different models: the *wave* model and the *particle* model (Englert et al., 1994).

Wave Model of Electromagnetic Energy

In the 1860s, James Clerk Maxwell (1831–1879) conceptualized electromagnetic radiation (EMR) as an electromagnetic wave that travels through space at the speed of light, *c*, which is 3 x 10^8 meters per second (hereafter referred to as m s^{-1}) or 186,282.03 miles s^{-1} (Trefil and Hazen, 1995). A useful relation for quick calculations is that light travels about 1 ft per nanosecond (10^{-9} s) (Rinker, 1999). The *electromagnetic wave* consists of two fluctuating fields — one electric and the other magnetic (Figure 2-2). The two vectors are at right angles (orthogonal) to one another, and both are perpendicular to the direction of travel (Bolemon, 1985).

But how is an electromagnetic wave created? *Electromagnetic radiation* is generated whenever an electrical charge is accelerated. The wavelength (λ) of the electromagnetic radiation depends upon the length of time that the charged particle is accelerated. Its frequency (ν) depends on the number of accelerations per second. *Wavelength* is formally defined as the mean distance between maximums (or minimums) of a roughly periodic pattern (Figure 2-2) and is normally measured in micrometers (μm) or nanometers (nm). *Frequency* is the number of wavelengths that pass a point per unit time. A wave that sends one crest by every second (completing one cycle) is said to have a frequency of one cycle per second, or one *hertz*, abbreviated 1 Hz. Frequently used measures of wavelength and frequency are found in Table 2-1.

The relationship between the wavelength (λ) and frequency (ν) of electromagnetic radiation is based on the following formula, where *c* is the speed of light (Egan, 1985):

$$c = \lambda\nu \qquad (2\text{-}1)$$

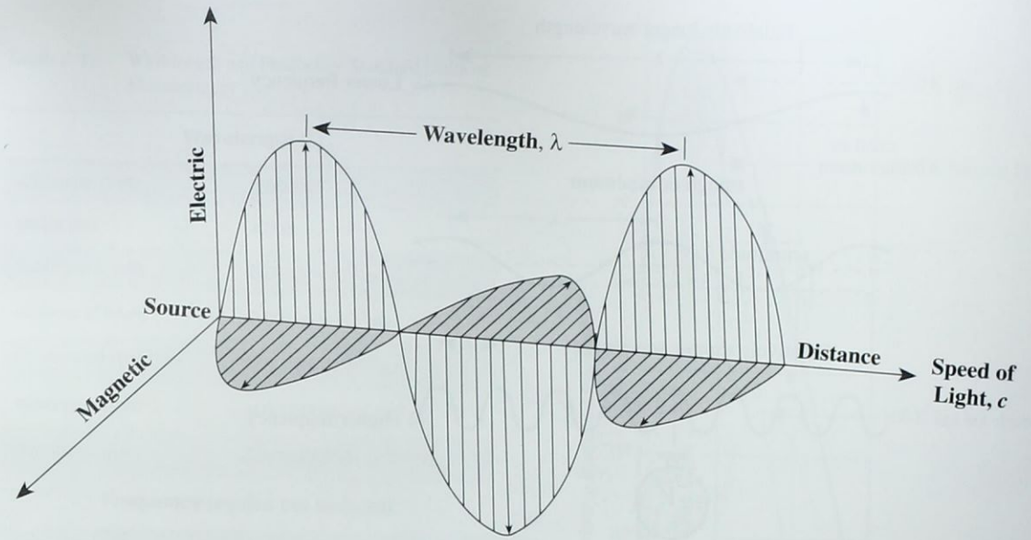

Figure 2-2 An electromagnetic wave is composed of both electric and magnetic vectors that are orthogonal (at 90° angles) to one another. The waves travel from the source at the speed of light (3 x 10^8 m s^{-1}).

$$\nu = \frac{c}{\lambda} \qquad (2\text{-}2)$$

and

$$\lambda = \frac{c}{\nu}. \qquad (2\text{-}3)$$

Note that frequency is *inversely* proportional to wavelength. This relationship is shown diagrammatically in Figure 2-3, where the longer the wavelength, the lower the frequency; the shorter the wavelength, the higher the frequency. When electromagnetic radiation passes from one substance to another, the speed of light and wavelength change while the frequency remains the same.

All objects above absolute zero (-273°C or 0 K) emit electromagnetic energy, including water, soil, rock, vegetation, and the surface of the Sun. The Sun represents the initial source of most of the electromagnetic energy recorded by remote sensing systems (except radar and sonar) (Figure 2-4; Color Plate 2-1). We may think of the Sun as a 6,000 K *blackbody* (a theoretical construct that absorbs and radiates energy at the maximum possible rate per unit area at each wavelength (λ) for a given temperature). The total emitted radiation from a blackbody (M_λ) measured in Watts per m^{-2} is proportional to the fourth power of its absolute temperature (*T*) measured in degrees Kelvin. This is known as the *Stefan-Boltzmann law* and is expressed as:

$$M_\lambda = \sigma T^4 \qquad (2\text{-}4)$$

where σ is the Stefan-Boltzmann constant, 5.6697 x 10^{-8}W $m^{-2}K^{-4}$. The important thing to remember is that the amount of energy emitted by an object such as the Sun or the Earth is a function of its temperature. The greater the temperature, the greater the amount of radiant energy exiting the object. The actual amount of energy emitted by an object is computed by summing (integrating) the area under its curve (Figure 2-5). It is clear from this illustration that the total emitted radiation from the 6,000 K Sun is far greater than that emitted by the 300 K Earth.

In addition to computing the total amount of energy exiting a theoretical blackbody such as the Sun, we can determine its dominant wavelength (λ_{max}) based on *Wien's displacement law*:

$$\lambda_{max} = \frac{k}{T} \qquad (2\text{-}5)$$

where *k* is a constant equaling 2898 μm K, and *T* is the absolute temperature in degrees Kelvin. Therefore, as the Sun

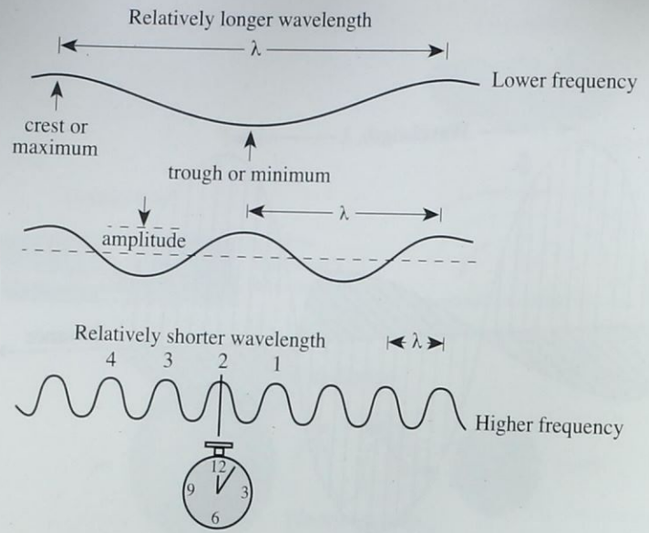

Figure 2-3 This cross-section of several electromagnetic waves illustrates the inverse relationship between wavelength (λ) and frequency (ν). The longer the wavelength, the lower the frequency; the shorter the wavelength, the higher the frequency. The amplitude of an electromagnetic wave is the height of the wave crest above the undisturbed position. Successive wave crests are numbered 1, 2, 3, and 4. An observer at the position of the clock records the number of crests that pass by in a second. This frequency is measured in cycles per second, or *hertz*.

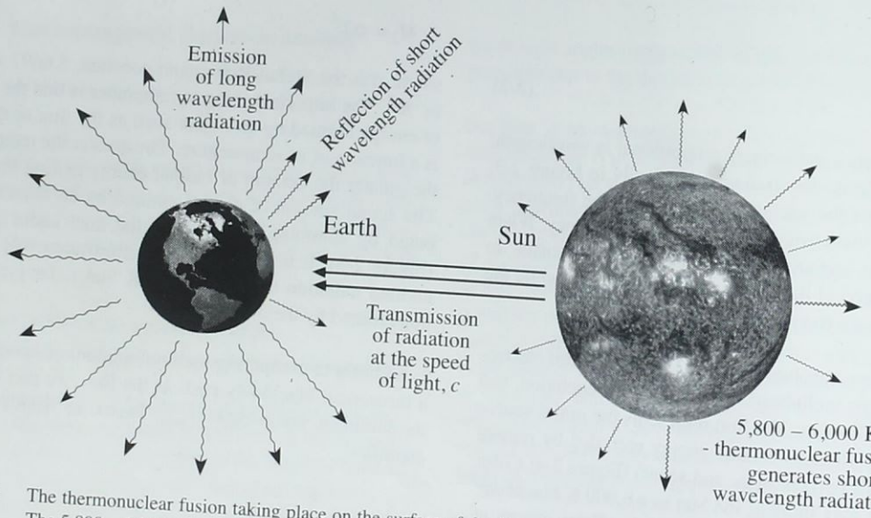

Figure 2-4 The thermonuclear fusion taking place on the surface of the Sun yields a continuous spectrum of electromagnetic energy. The 5,800 – 6,000 K temperature of this process produces a large amount of relatively short wavelength energy that travels through the vacuum of space at the speed of light. Some of this energy is intercepted by the Earth, where it interacts with the atmosphere and surface materials. The Earth reflects some of the energy directly back out to space or it may absorb the short wavelength energy and then reemit it at a longer wavelength (after Strahler and Strahler, 1989). This process takes place continually .

Table 2-1. Wavelength and Frequency Standard Units of Measurement

Wavelength (λ)	
kilometer (km)	1,000 m
meter (m)	1.0 m
centimeter (cm)	0.01 m = 10^{-2} m
millimeter (mm)	0.001 m = 10^{-3} m
micrometer (μm)	0.000001 = 10^{-6} m
nanometer (nm)	0.000000001 = 10^{-9} m
Angstrom (A)	0.0000000001 = 10^{-10} m
Frequency (cycles per second)	
hertz (Hz)	1
kilohertz (kHz)	1,000 = 10^{3}
megahertz (MHz)	1,000,000 = 10^{6}
gigahertz (GHz)	1,000,000,000 = 10^{9}

approximates a 6,000 K blackbody, its dominant wavelength (λ_{max}) is 0.48 μm:

$$0.483\mu m = \frac{2898\ \mu m\ K}{6000\ K}.$$

Electromagnetic energy from the Sun travels in eight minutes across the intervening 93 million miles (150 million kilometers) of space to the Earth. As shown in Figure 2-5, the Earth approximates a 300 K (27°C) blackbody and has a dominant wavelength at approximately 9.66 μm:

$$9.66\mu m = \frac{2898\ \mu m\ K}{300\ K}.$$

Although the Sun has a dominant wavelength at 0.48 μm, it produces a continuous spectrum with electromagnetic radiation ranging from very short, extremely high frequency gamma and cosmic waves to long, very low frequency radio waves (Figures 2-6 and 2-7). The Earth only intercepts a very small portion of the electromagnetic energy produced by the Sun.

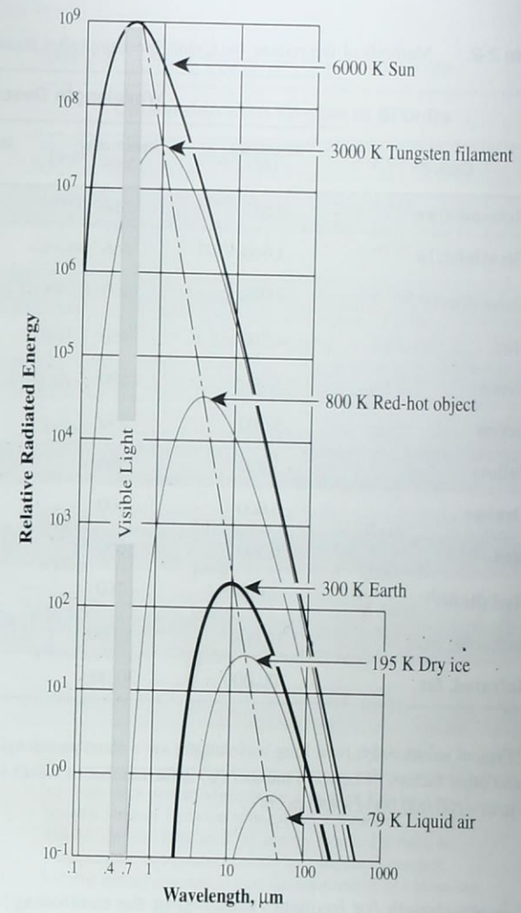

Figure 2-5 Blackbody radiation curves for several objects, including the Sun and the Earth, which approximate 6,000 K and 300 K blackbodies, respectively. The area under each curve may be summed to compute the total radiant energy (M_λ) exiting each object (Equation 2-4). Thus, the Sun produces more radiant exitance than the Earth because its temperature is greater. As the temperature of an object increases, its dominant wavelength (λ_{max}) shifts toward the shorter wavelengths of the electromagnetic spectrum.

As mentioned in Chapter 1, in remote sensing research we often specify a particular region of the electromagnetic spectrum (e.g., red light) by identifying a beginning and ending wavelength (or frequency) and then attaching a description.

Table 2-2. Methods of Describing the Color Spectrum (after Nassau, 1983)

Color[a]	Wavelength Descriptions					Energy Descriptions
	Angstrom (A)	Nanometer (nm)	Micrometer (μm)	Frequency Hz (x 1014)	Wave Number[c] (ψ cm^{-1})	Electron Volt (eV)
Ultraviolet, sw	2,537	254	0.254	11.82	39,400	4.89
Ultraviolet, lw	3,660	366	0.366	8.19	27,300	3.39
Violet (limit)[b]	4,000	400	0.40	7.50	25,000	3.10
Blue	4,500	450	0.45	6.66	22,200	2.75
Green	5,000	500	0.50	6.00	20,000	2.48
Green	5,500	550	0.55	5.45	18,200	2.25
Yellow	5,800	580	0.58	5.17	17,240	2.14
Orange	6,000	600	0.60	5.00	16,700	2.06
Red	6,500	650	0.65	4.62	15,400	1.91
Red (limit)[b]	7,000	700	0.70	4.29	14,300	1.77
Infrared, near	10,000	1,000	1.0	3.00	10,000	1.24
Infrared, far	300,000	30,000	30.00	0.10	333	0.041

[a]Typical values only; lw = long wavelength; sw = short wavelength. [b]Exact limit depends on the observer, light intensity, eye adaptation, and other factors. [c]The wave number (ψ) is the number of waves in a unit length (usually per cm). Therefore, $\psi = 1 / \lambda$ (cm) = 10,000 / λ (μm) =100,000,000 / λ (A) in cm^{-1}.

This wavelength (or frequency) interval in the electromagnetic spectrum is commonly referred to as a *band*, *channel*, or *region*. The major subdivisions of visible light are presented diagrammatically in Figure 2-7 and summarized in Table 2-2. For example, we generally think of visible light as being composed of energy in the blue (0.4 – 0.5 μm), green (0.5 – 0.6 μm), and red (0.6 – 0.7 μm) bands of the electromagnetic spectrum (Sagan, 1994). Similarly, reflected near-infrared energy in the region from 0.7 – 1.3 μm is commonly used to expose black-and-white and color-infrared sensitive film.

The middle-infrared region includes energy with a wavelength of 1.3 – 3 μm. The thermal infrared region has two very useful bands at 3 – 5 μm and 8 – 14 μm. The microwave portion of the spectrum consists of much longer wavelengths (1 mm – 1 m). The radio-wave portion of the spectrum may be subdivided into UHF, VHF, Radio (HF), LF, and ULF frequencies.

The spectral resolution of most remote sensing systems is described in terms of bands of the electromagnetic spectrum. For example, the spectral dimensions of the four bands of the Landsat Multispectral Scanner (MSS) and SPOT High Resolution Visible (HRV) sensors are shown in Figure 2-8, along with the spatial resolution of each band for comparison. The exact Landsat MSS and SPOT HRV band specifications are found in Chapter 7.

Electromagnetic energy may be described not only in terms of wavelength and frequency but also in photon energy units such as Joules (J) and electron volts (eV), as shown in Figure 2-7. Several of the more important mass, energy, and power conversions are summarized in Table 2-3.

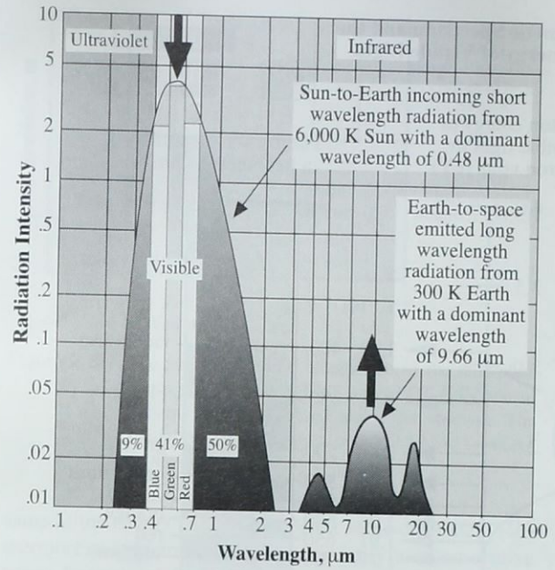

Figure 2-6 The Sun approximates a 6,000 K blackbody with a dominant wavelength of about 0.48 μm. The Earth approximates a 300 K blackbody with a dominant wavelength of about 9.66 μm. The 6,000 K Sun produces approximately 41 percent of its energy in the visible region from 0.4 – 0.7 μm (blue, green, and red light). The other 59 percent of the energy is in wavelengths shorter than blue light (<0.4 μm) and longer than red light (>0.7 μm). Our eyes are only sensitive to light from 0.4 to 0.7 μm (after Strahler and Strahler, 1989). Fortunately, it is possible to make remote sensor detectors that are sensitive to energy in these nonvisible regions of the spectrum.

Table 2-3. Mass, Energy and Power Conversions

Conversion from English to SI Units

To get:	Multiply:	By:
newtons[a]	pounds	4.448
joules[b]	BTUs[c]	1055
joules	calories[d]	4.184
joules	kilowatt-hours[e]	3.6 x 10^6
joules	foot-pounds[f]	1.356
joules	horsepower[g]	745.7

Conversion from SI to English Units

To get:	Multiply:	By:
BTUs	joules	0.00095
calories	joules	0.2390
kilowatt-hours	joules	2.78 x 10^{-7}
foot-pounds	joules	0.7375
horsepower	watts	0.00134

[a]newton: force needed to accelerate a mass of 1 kg by 1 m s^{-2}
[b]joule: a force of 1 newton acting through 1 meter.
[c]British Thermal Unit, or BTU: energy required to raise the temperature of 1 pound of water by 1 degree Fahrenheit.
[d]calorie: energy required to raise the temperature of 1 kilogram of water by 1 degree Celsius.
[e]kilowatt-hour: 1000 joules per second for 1 hour.
[f]foot-pound: a force of 1 pound acting through 1 foot.
[g]horsepower: 550 foot-pounds per second.

The Particle Model - Radiation from Atomic Structures

In *Opticks* (1704), Sir Isaac Newton stated that light was a stream of particles, or corpuscles, traveling in straight lines. He also knew that light had wavelike characteristics based on his work with glass plates. Nevertheless, during the hundred years before 1905, light was thought of primarily as a smooth and continuous wave. Then, Albert Einstein (1879–1955) found that when light interacts with electrons, it has a different character. He concluded that when light interacts with matter, it behaves as though it is composed of many individual bodies called *photons*, which carry such particle-like properties as energy and momentum (Bolemon, 1985; Meadows, 1992). As a result, most physicists today would answer the question, What is light? by saying that light is a *particular* kind of matter (Feinberg, 1985). Thus, we sometimes describe electromagnetic energy in terms of its wavelike properties. But when the energy interacts with matter, it is useful to describe it as discrete packets of energy, or *quanta*. It is practical to review how electromagnetic energy is generated at the atomic level, as this provides insight as to how light interacts with matter.

Electrons are the tiny negatively charged particles that move around the positively charged nucleus of an atom (Figure 2-9). Atoms of different substances are made up of varying numbers of electrons arranged in different ways. The inter-

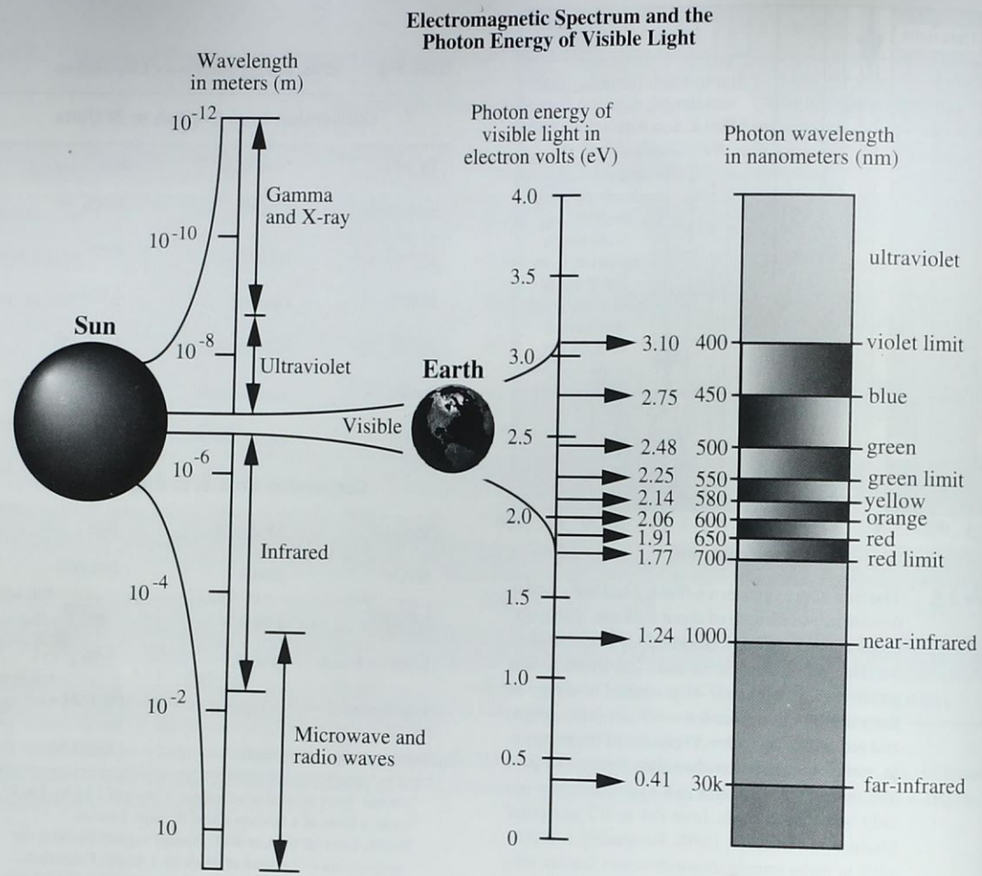

Figure 2-7 The electromagnetic spectrum and the photon energy of visible light. The Sun produces a continuous spectrum of energy from gamma rays to radio waves that continually bathe the Earth in energy. The visible portion of the spectrum may be measured using wavelength (measured in micrometers or nanometers, i.e., μm or nm) or electron volts (eV). All units are interchangeable.

action between the positively charged nucleus and the negatively charged electron keeps the electron in orbit. While its orbit is not explicitly fixed, each electron's motion is restricted to a definite range from the nucleus. The allowable orbital paths of electrons moving around an atom might be thought of as energy classes or levels (Figure 2-9a). In order for an electron to climb to a higher class, work must be performed. However, unless an amount of energy is available to move the electron up at least one energy level, it will accept no work. If a sufficient amount of energy is received, the electron will jump to a new level and the atom is said to be *excited* (Figure 2-9b). Once an electron is in a higher orbit, it possesses potential energy. After about 10^{-8} seconds, the electron falls back to the atom's lowest empty energy level or orbit and gives off radiation (Figure 2-9c). The wavelength of radiation given off is a function of the amount of work done on the atom, i.e., the quantum of energy it absorbed to cause the electron to become excited and move to a higher orbit.

Electron orbits are like the rungs of a ladder. Adding energy moves the electron up the energy ladder; emitting energy moves it down. However, the energy ladder differs from an ordinary ladder in that its rungs are unevenly spaced. This means that the energy an electron needs to absorb, or to give up, in order to jump from one orbit to the next may not be the

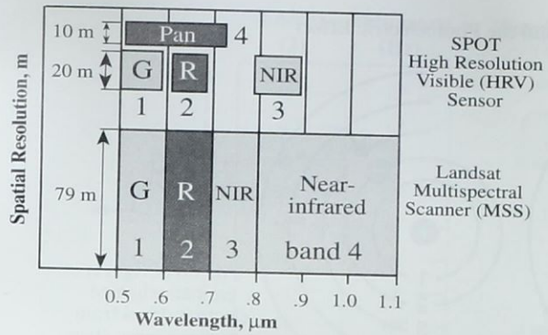

Figure 2-8 The nominal spectral bandwidths of the individual bands of the Landsat MSS and SPOT HRV sensor systems are summarized along the abscissa. The spatial resolution of each individual band is shown on the ordinate axis.

same as the energy change needed for some other step. Furthermore, an electron does not necessarily use consecutive rungs. Instead, it follows what physicists call *selection rules*. In many cases, an electron uses one sequence of rungs as it climbs the ladder and another sequence as it descends (Nassau, 1983). The energy that is left over when the electrically charged electron moves from an excited state (Figure 2-9b) to a de-excited state (Figure 2-9c) is emitted by the atom as a single packet of electromagnetic radiation; a particle-like unit of light called a *photon*. Every time an electron jumps from a higher to a lower energy level, a photon moves away at the speed of light.

Somehow an electron must disappear from its original orbit and reappear in its destination orbit without ever having to traverse any of the positions in between. This process is called a *quantum leap* or *quantum jump*. If the electron leaps from its highest excited state to the ground state in a single leap, it will emit a single photon of energy. It is also possible for the electron to leap from an excited orbit to the ground state in a series of jumps, e.g., from 4 to 2 to 1. If it takes two leaps to get to the ground state, then each of these jumps will emit photons of somewhat less energy. The energies emitted in the two different jumps must sum to the total of the single large jump (Trefil and Hazen, 1995).

Niels Bohr (1885–1962) and Max Planck recognized the discrete nature of exchanges of radiant energy and proposed the *quantum theory* of electromagnetic radiation. This theory states that energy is transferred in discrete packets called quanta or photons as discussed. The relationship between the frequency of radiation expressed by wave theory and the quantum is (Bolemon, 1985):

$$Q = h\nu \tag{2-6}$$

where Q is the energy of a quantum measured in Joules (J), h is the Planck constant (6.626×10^{-34} J s), and ν is the frequency of the radiation. Referring to Equation 2-3, we can multiply the equation by h/h, or 1, without changing its value:

$$\lambda = \frac{hc}{h\nu}. \tag{2-7}$$

By substituting Q for $h\nu$ (from Equation 2-6) we can express the wavelength associated with a quantum of energy as:

$$\lambda = \frac{hc}{Q} \tag{2-8}$$

or

$$Q = \frac{hc}{\lambda}. \tag{2-9}$$

Thus, we see that the energy of a quantum is inversely proportional to its wavelength, i.e., the longer the wavelength involved, the lower its energy content. This inverse relationship is important to remote sensing because it suggests that it is more difficult to detect longer wavelength energy being emitted at thermal infrared wavelengths than those at shorter visible wavelengths. In fact, it might be necessary to have the sensor look at or dwell longer on the parcel of ground if we are trying to measure the longer wavelength energy. The energy of quanta (photons) ranging from gamma rays to radio waves is summarized in Figure 2-10.

Substances have color because of differences in their energy levels and the selection rules. For example, consider energized sodium vapor that produces a bright yellow light that is used in some street lamps. When a sodium vapor lamp is turned on, several thousand volts of electricity energize the vapor. The outermost electron in each energized atom of sodium vapor climbs to a higher rung on the energy ladder and then returns down the ladder in a certain sequence of rungs, the last two of which are 2.1 eV apart (Figure 2-11). The energy released in this last leap appears as a photon of yellow light with a wavelength of 0.58 μm with 2.1 eV of energy (Nassau, 1983).

Matter can be heated to such high temperatures that electrons that normally move in captured, nonradiating orbits break free (Figure 2-9d). When this happens, the atom remains with a positive charge equal to the negatively charged electron that escaped. The electron becomes a free

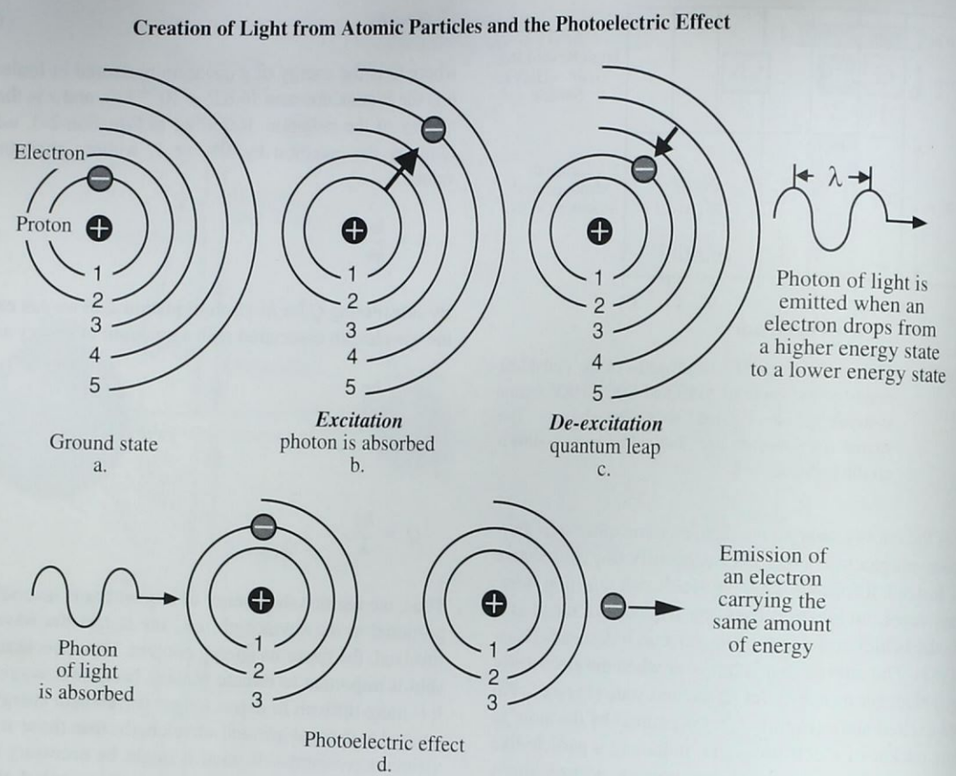

Figure 2-9 a–c) A photon of electromagnetic energy is emitted when an electron in an atom or molecule drops from a higher energy state to a lower energy state. The light emitted (i.e., its wavelength) is a function of the changes in the energy levels of the outer, valence electron. For example, yellow light is produced from a sodium vapor lamp in Figure 2-11. d) Matter can also be subjected to such high temperatures that electrons that normally move in captured, nonradiating orbits are broken free. When this happens, the atom remains with a positive charge equal to the negatively charged electron which escaped. The electron becomes a free electron, and the atom is called an ion. If another free electron fills the vacant energy level created by the free electron, then radiation from all wavelengths is produced, i.e., a continuous spectrum of energy. The intense heat at the surface of the Sun produces a continuous spectrum in this manner.

electron and the atom is called an *ion*. In the ultraviolet and visible (blue, green, and red) parts of the electromagnetic spectrum, radiation is produced by changes in the energy levels of the outer valence electrons. The wavelengths of energy produced are a function of the particular orbital levels of the electrons involved in the excitation process. If the atoms absorb enough energy to become ionized and if a free electron drops in to fill the vacant energy level, then the radiation given off is unquantized and a *continuous spectrum* is produced rather than a band or a series of bands. Every encounter of one of the free electrons with a positively charged nucleus causes rapidly changing electric and magnetic fields, so that radiation at all wavelengths is produced.

The hot surface of the Sun is largely a *plasma* in which radiation of all wavelengths is produced. As previously shown in Figure 2- 7, the spectra of a plasma like the Sun is a continuous spectrum.

In atoms and molecules, electron orbital changes produce the shortest wavelength radiation, molecule vibrational motion changes produce near- and/or middle-infrared energy, and rotational motion changes produce long wavelength infrared or microwave radiation. More will be said about how thermal infrared radiation is produced and recorded by remote sensing systems in Chapter 8 (Thermal Infrared Remote Sensing).

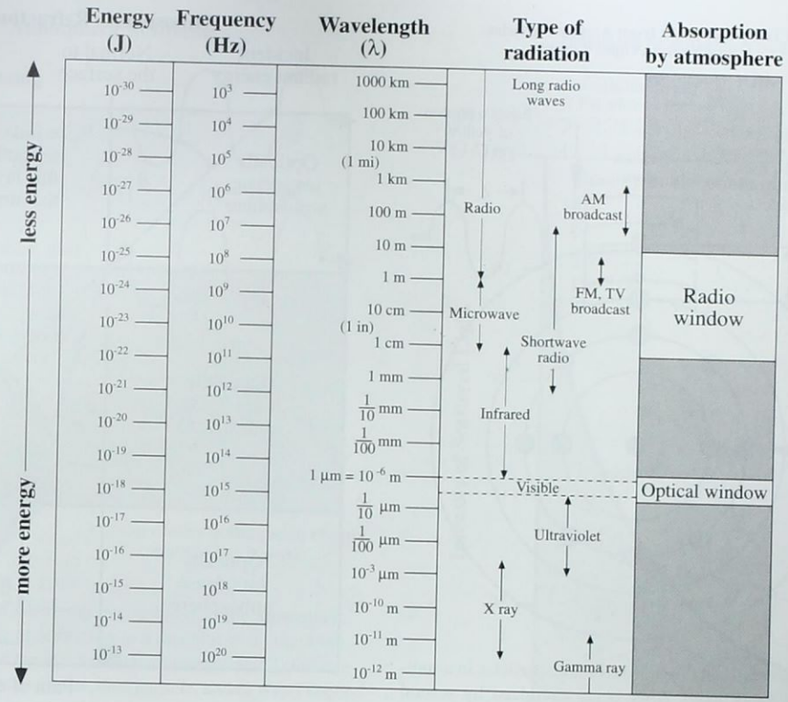

Figure 2-10 The energy of quanta (photons) ranging from gamma rays to radio waves in the electromagnetic spectrum.

Energy-Matter Interactions in the Atmosphere

Radiant energy is the capacity of radiation within a spectral band to do work (Colwell, 1983). Once electromagnetic radiation is generated, it is propagated through the Earth's atmosphere almost at the speed of light in a vacuum. Unlike a vacuum in which nothing happens, however, the atmosphere may affect not only the speed of radiation but also its wavelength, its intensity, and its spectral distribution. The electromagnetic radiation may also be diverted from its original direction due to refraction.

Refraction

The speed of light in a vacuum is 3×10^8 m s^{-1}. When electromagnetic radiation (EMR) encounters substances of different density, like air and water, refraction may take place. *Refraction* refers to the bending of light when it passes from one medium to another. Refraction occurs because the media are of differing densities and the speed of EMR is different in each. The *index of refraction (n)* is a measure of the optical density of a substance. This index is the ratio of the speed of light in a vacuum, c, to the speed of light in a substance such as the atmosphere or water, c_n (Mulligan, 1980):

$$n = \frac{c}{c_n}. \qquad (2\text{-}10)$$

The speed of light in a substance can never reach the speed of light in a vacuum. Therefore, its index of refraction must always be greater than 1. For example, the index of refraction for the atmosphere is 1.0002926 and 1.33 for water. Light travels more slowly through water.

Refraction can be described by Snell's law, which states that for a given frequency of light (we must use frequency since, unlike wavelength, it does not change when the speed of light changes), the product of the index of refraction and the sine of the angle between the ray and a line normal to the interface is constant:

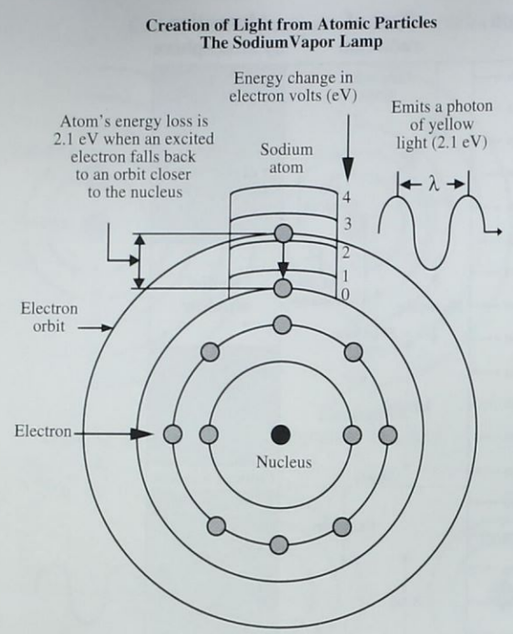

Figure 2-11 The creation of light from atomic particles in a sodium vapor lamp. After being energized by several thousand volts of electricity, the outermost electron in each energized atom of sodium vapor climbs to a high rung on the energy ladder and then returns down the ladder in a predictable fashion. The last two rungs in the descent are 2.1 eV apart. This produces a photon of yellow light which has 2.1 eV of energy (refer to Figure 2-7 and Table 2-2).

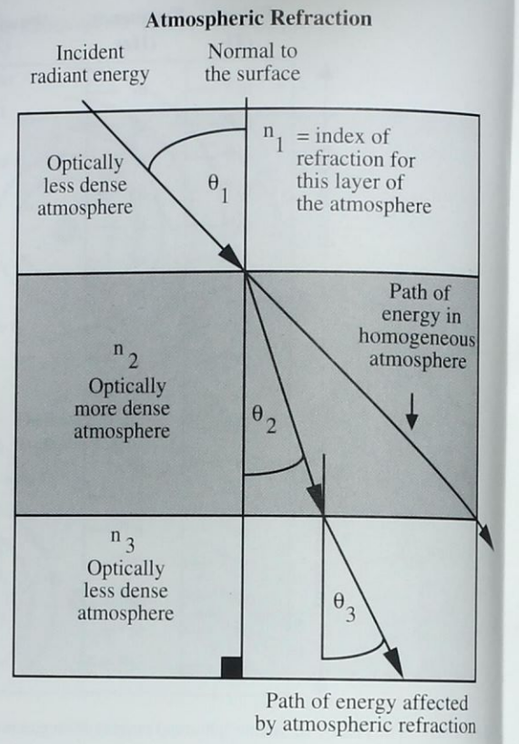

Figure 2-12 Refraction in three nonturbulent atmospheric layers. The incident energy is bent from its normal trajectory as it travels from one atmospheric layer to another. Snell's law can be used to predict how much bending will take place, based on a knowledge of the angle of incidence (θ) and the index of refraction of each atmospheric level, n_1, n_2, n_3.

$$n_1 \sin\theta_1 = n_2 \sin\theta_2 . \qquad (2\text{-}11)$$

From Figure 2-12 we can see that a nonturbulent atmosphere can be thought of as a series of layers of gases, each with a different density. Anytime energy is propagated through the atmosphere for any appreciable distance at any angle other than vertical, refraction occurs.

The amount of refraction is a function of the angle made with the vertical (θ), the distance involved (in the atmosphere the greater the distance, the more changes in density), and the density of the air involved (air is usually more dense near sea level). Serious errors in location due to refraction can occur in images formed from energy detected at high altitudes or at acute angles. However, these location errors are predictable by Snell's law and thus can be removed. Notice that

$$\sin\theta_2 = \frac{n_1 \sin\theta_1}{n_2} . \qquad (2\text{-}12)$$

Therefore, if one knows the index of refraction of medium n_1 and n_2 and the angle of incidence of the energy to medium n_1, it is possible to predict the amount of refraction that will take place *(sin θ_2)* in medium n_2 using trigonometric relationships.

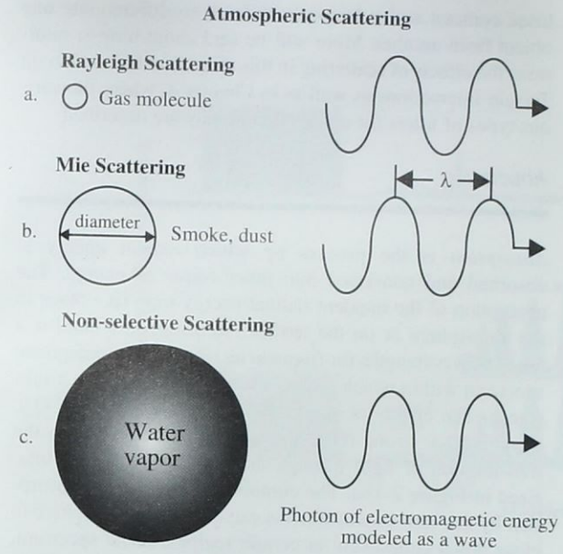

Figure 2-13 Types of scattering encountered in the atmosphere. The type of scattering is a function of 1) the wavelength of the incident radiant energy, and 2) the size of the gas molecule, dust particle, and/or water vapor droplet encountered.

Scattering

One very serious effect of the atmosphere is the scattering of radiation by atmospheric particles. *Scattering* differs from reflection in that the direction associated with scattering is unpredictable, whereas the direction of reflection (to be defined shortly) is predictable. There are essentially three types of scattering: Rayleigh, Mie, and Non-selective scattering. The relative size of the wavelength of the incident electromagnetic radiation, the diameter of the gases, water vapor, and/or dust with which the energy interacts, and the type of scattering which should occur are summarized in Figure 2-13.

Rayleigh scattering (sometimes referred to as molecular scattering) occurs when the effective diameter of the matter (usually air molecules such as oxygen and nitrogen in the atmosphere) are many times smaller (usually < 0.1) than the wavelength of the incident electromagnetic radiation (Figure 2-13a). Rayleigh scattering is named after the English physicist Lord Rayleigh who offered the first coherent explanation for it (Sagan, 1994). All scattering is accomplished through absorption and reemission of radiation by atoms or molecules in the manner described in the section on radiation from atomic structures. It is impossible to predict the direction in which a specific atom or molecule will emit a photon, hence scattering. The energy required to excite an atom is associated with powerful short-wavelength, high-frequency radiation. The amount of scattering is inversely related to the fourth power of the radiation's wavelength. For example, ultraviolet light at 0.3 μm is scattered approximately 16 times more than red light at 0.6 μm, i.e., $[(0.6/0.3)^4 = 16]$. Blue light at 0.4 μm is scattered about 5 times that of red light at 0.6 μm, i.e., $[(0.6/0.4)^4 = 5.06]$. The amount of Rayleigh scattering expected throughout the visible spectrum (0.4 – 0.7 μm) is shown in Figure 2-14.

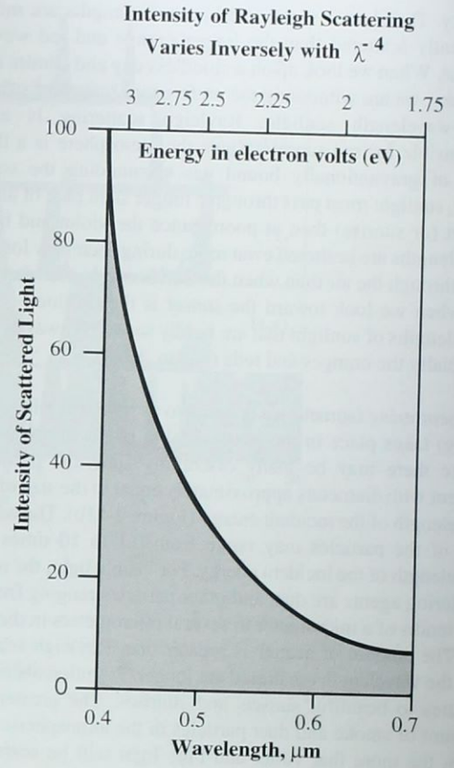

Figure 2-14 The intensity of Rayleigh scattering varies inversely with the fourth power of the wavelength (λ^{-4}).

Most Rayleigh scattering takes place in the upper 4.5 km of the atmosphere. It is responsible for the blue appearance of

the sky. The shorter violet and blue wavelengths are more efficiently scattered than the longer orange and red wavelengths. When we look up on a cloudless day and admire the blue sky, we are witnessing the preferential scattering of the short-wavelength sunlight. Rayleigh scattering is also responsible for red sunsets. Since the atmosphere is a thin shell of gravitationally bound gas surrounding the solid Earth, sunlight must pass through a longer slant path of air at sunset (or sunrise) than at noon. Since the violet and blue wavelengths are scattered even more during their now longer path through the air than when the Sun is overhead, what we see when we look toward the sunset is the residue — the wavelengths of sunlight that are hardly scattered away at all, especially the oranges and reds (Sagan, 1994).

Mie scattering (sometimes referred to as nonmolecular scattering) takes place in the lower 4.5 km of the atmosphere, where there may be many essentially spherical particles present with diameters approximately equal to the size of the wavelength of the incident energy (Figure 2-13b). The actual size of the particles may range from 0.1 to 10 times the wavelength of the incident energy. For visible light, the main scattering agents are dust and other particles ranging from a few tenths of a micrometer to several micrometers in diameter. The amount of scatter is greater than Rayleigh scatter, and the wavelengths scattered are longer. Pollution also contributes to beautiful sunsets and sunrises. The greater the amount of smoke and dust particles in the atmospheric column, the more that violet and blue light will be scattered away and only the longer orange and red wavelength light will reach our eyes.

Non-selective scattering takes place in the lowest portions of the atmosphere where there are particles greater than 10 times the wavelength of the incident electromagnetic radiation (Figure 2-13c). This type of scattering is non-selective, i.e., all wavelengths of light are scattered, not just blue, green, or red. Thus, the water droplets and ice crystals that make up clouds and fog banks scatter all wavelengths of visible light equally well, causing the cloud to appear white. Non-selective scattering of approximately equal proportions of blue, green, and red light always appears as white light to the casual observer. This is the reason why putting our automobile high beams on in fog only makes the problem worse as we non-selectively scatter even more light into our visual field of view.

Scattering is a very important consideration in remote sensing investigations. It can severely reduce the information content of remotely sensed data to the point that the imagery loses contrast and it becomes difficult to differentiate one object from another. More will be said about how to minimize the effects of scattering in this chapter in the section on Terrain Interactions as well as in Chapter 4, where the various types of filters for aerial photography are described.

Absorption

Absorption is the process by which radiant energy is absorbed and converted into other forms of energy. The absorption of the incident radiant energy may take place in the atmosphere or on the terrain. An *absorption band* is a range of wavelengths (or frequencies) in the electromagnetic spectrum within which radiant energy is absorbed by a substance. The effects of water (H_2O), carbon dioxide (CO_2), oxygen (O_2), ozone (O_3), and nitrous oxide (N_2O) on the transmission of light through the atmosphere are summarized in Figure 2-15a. The cumulative effect of the absorption by the various constituents can cause the atmosphere to close down completely in certain regions of the spectrum. This is very bad for remote sensing because no energy is available to be sensed. Conversely, in the visible portion of the spectrum (0.4 – 0.7 μm), the atmosphere does not absorb all of the incident energy but transmits it rather effectively. Portions of the spectrum that transmit radiant energy effectively are called *atmospheric windows*.

Absorption occurs when incident energy of the same frequency as the resonant frequency of an atom or molecule is absorbed, producing an excited state. If instead of reradiating a photon of the same wavelength, the energy is transformed into heat motion and is subsequently reradiated at a longer wavelength, absorption occurs. When dealing with a medium like air, absorption and scattering are frequently combined into an *extinction coefficient*. Transmission is inversely related to the extinction coefficient times the thickness of the layer. Certain wavelengths of radiation are affected far more by absorption than by scattering. This is particularly true of infrared and wavelengths shorter than visible light. The combined effects of atmospheric absorption, scattering, and reflectance (from cloud tops) can dramatically reduce the amount of solar radiation reaching the Earth's surface at sea level as shown in Figure 2-15b.

Chlorophyll in vegetation absorbs much of the incident blue and red light for photosynthetic purposes. Chapter 10 describes the importance of these chlorophyll absorption bands and their role when remotely sensing vegetation. Similarly, water is an excellent absorber of energy (Chapter 11).

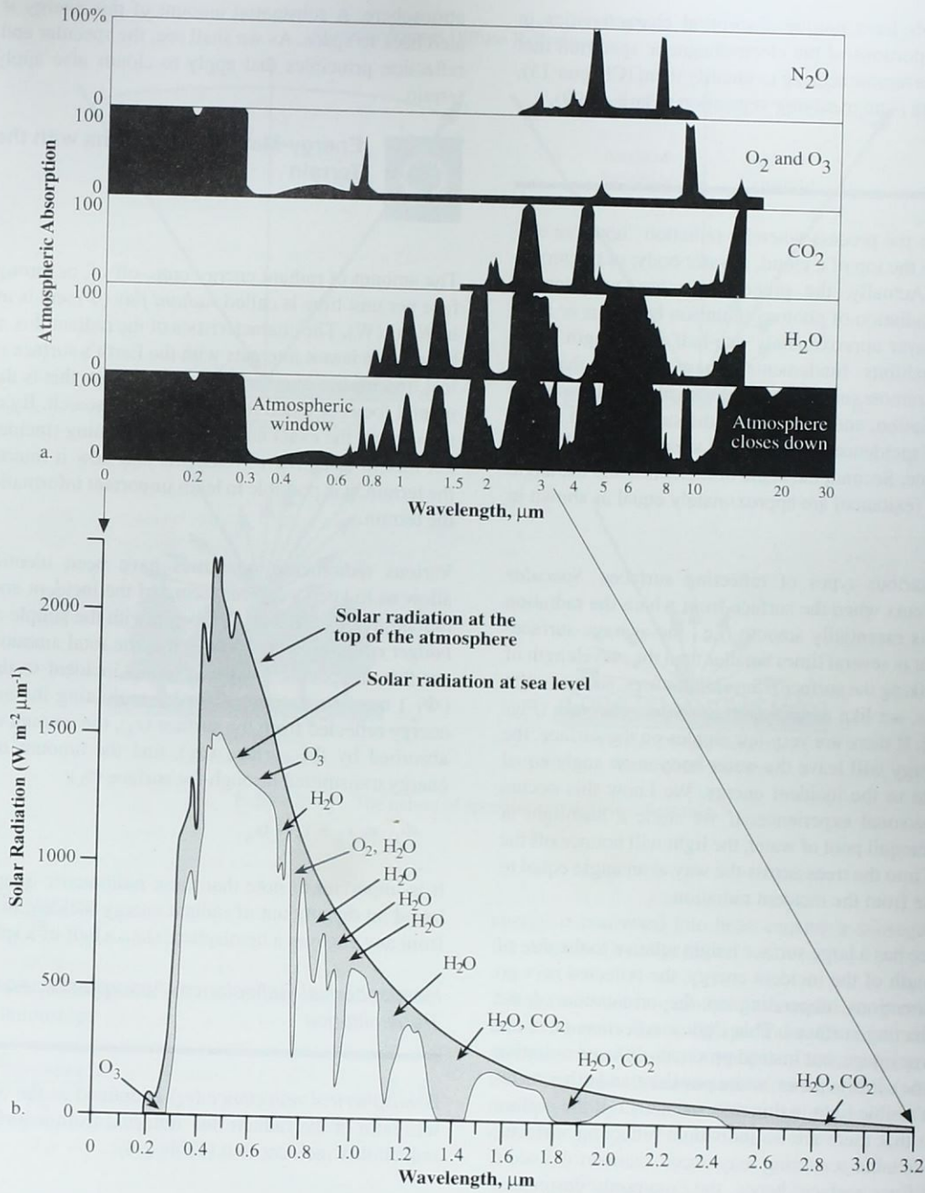

Figure 2-15 a) The absorption of the Sun's incident electromagnetic energy in the region from 0.1 – 30 μm by various atmospheric gases. The first four graphs depict the absorption characteristics of N_2O, O_2 and O_3, CO_2, and H_2O, while the final graphic depicts the cumulative result of having all these constituents in the atmosphere at one time. The atmosphere essentially "closes down" in certain portions of the spectrum while "atmospheric windows" exist in other regions that transmit incident energy effectively to the ground. It is within these windows that remote sensing systems must function. b) The combined effects of atmospheric absorption, scattering and reflectance reduce the amount of solar irradiance reaching the Earth's surface at sea level (after Slater, 1980).

Many minerals have unique absorption characteristics in very specific portions of the electromagnetic spectrum that allow us to use remote sensing to identify them (Chapter 13), assuming there is no overlying vegetation (Clark, 1999).

Reflectance

Reflectance is the process whereby radiation "bounces off" an object like the top of a cloud, a water body, or the terrestrial Earth. Actually, the process is more complicated, involving reradiation of photons in unison by atoms or molecules in a layer approximately one-half wavelength deep. Reflection exhibits fundamental characteristics that are important in remote sensing. First, the incident radiation, the reflected radiation, and a vertical to the surface from which the angles of incidence and reflection are measured all lie in the same plane. Second, the angle of incidence and the angle of reflection (exitance) are approximately equal as shown in Figure 2-16.

There are various types of reflecting surfaces. *Specular reflection* occurs when the surface from which the radiation is reflected is essentially smooth (i.e., the average surface-profile height is several times smaller than the wavelength of radiation striking the surface). Several features, such as calm water bodies, act like *near-perfect specular reflectors* (Figure 2-16a,b). If there are very few ripples on the surface, the incident energy will leave the water body at an angle equal and opposite to the incident energy. We know this occurs from our personal experience. If we shine a flashlight at night on a tranquil pool of water, the light will bounce off the surface and into the trees across the way at an angle equal to and opposite from the incident radiation.

If the surface has a large surface height relative to the size of the wavelength of the incident energy, the reflected rays go in many directions, depending on the orientation of the smaller reflecting surfaces. This *diffuse reflection* does not yield a mirror image, but instead produces diffused radiation (Figure 2-16c). White paper, white powders, and other materials reflect visible light in this diffuse manner. If the surface is so rough that there are no individual reflecting surfaces, then unpredictable scattering may occur. Lambert defined a perfectly diffuse surface; hence, the commonly designated *Lambertian surface* is one for which the radiant flux leaving the surface is constant for any angle of reflectance to the surface (Figure 2-16d).

A considerable amount of incident radiant flux from the Sun is reflected from the tops of clouds and other materials in the atmosphere. A substantial amount of this energy is reradiated back to space. As we shall see, the specular and diffuse reflection principles that apply to clouds also apply to the terrain.

Energy-Matter Interactions with the Terrain

The amount of radiant energy onto, off of, or through a surface per unit time is called *radiant flux* (Φ) and is measured in Watts (W). The characteristics of the radiant flux and what happens to it as it interacts with the Earth's surface is of critical importance in remote sensing. In fact, this is the fundamental focus of much remote sensing research. By carefully monitoring the exact nature of the incoming (incident) radiant flux in selective wavelengths and how it interacts with the terrain, it is possible to learn important information about the terrain.

Various radiometric quantities have been identified that allow us to keep a careful record of the incident and exiting radiant flux (Table 2-4). We begin with the simple *radiation budget equation,* which states that the total amount of radiant flux in specific wavelengths (λ) incident to the terrain (Φ_{i_λ}) must be accounted for by evaluating the amount of energy reflected from the surface (r_λ), the amount of energy absorbed by the surface (α_λ), and the amount of radiant energy transmitted through the surface (τ_λ):

$$\Phi_{i_\lambda} = r_\lambda + \tau_\lambda + \alpha_\lambda . \tag{2-13}$$

It is important to note that these radiometric quantities are based on the amount of radiant energy incident to a surface from any angle in a hemisphere (i.e., a half of a sphere).

Hemispherical Reflectance, Absorptance, and Transmittance

Hemispherical reflectance (r_λ) is defined as the dimensionless ratio of the radiant flux reflected from a surface to the radiant flux incident to it (Table 2-4):

$$r_\lambda = \frac{\Phi_{reflected}}{\Phi_{i_\lambda}} . \tag{2-14}$$

Hemispherical transmittance (τ_λ) is defined as the dimensionless ratio of the radiant flux transmitted through a surface to the radiant flux incident to it:

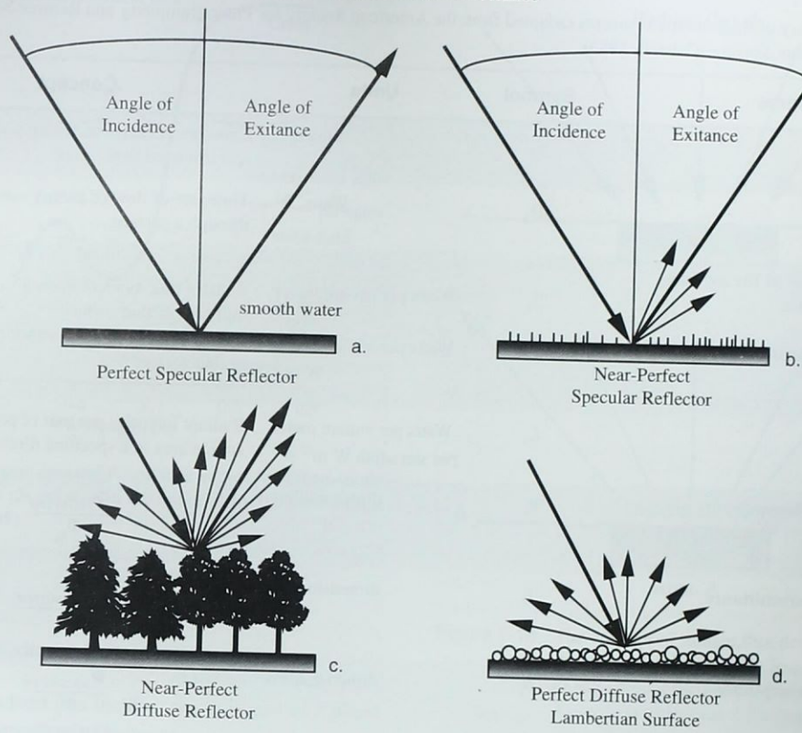

Figure 2-16 The nature of specular and diffuse reflectance.

$$\tau_\lambda = \frac{\Phi_{transmitted}}{\Phi_{i_\lambda}} . \tag{2-15}$$

Hemispherical absorptance (α_λ) is defined by the dimensionless relationship:

$$\alpha_\lambda = \frac{\Phi_{absorbed}}{\Phi_{i_\lambda}} \tag{2-16}$$

or

$$\alpha_\lambda = 1 - (r_\lambda + \tau_\lambda) . \tag{2-17}$$

These definitions imply that radiant energy must be conserved, i.e., it is either returned back by reflection, transmitted through a material, or absorbed and transformed into some other form of energy inside the terrain. The net effect of absorption of radiation by most substances is that the energy is converted into heat, causing a subsequent rise in the substance's temperature.

These radiometric quantities are useful for producing general statements about the spectral reflectance, absorptance, and transmittance characteristics of terrain features. In fact, if we take the simple hemispherical reflectance equation and multiply it by 100, we obtain an expression for percent reflectance (p_{r_λ}):

$$p_{r_\lambda} = \frac{\Phi_{reflected}}{\Phi_{i_\lambda}} \times 100 \tag{2-18}$$

which is often used in remote sensing research to describe the spectral reflectance characteristics of various phenomena. Examples of spectral reflectance curves for selected urban-suburban phenomena are shown in Figure 2-17. Spectral reflectance curves typically provide no information

Table 2-4. Summary of Radiometric Concepts (adapted from the American Society for Photogrammetry and Remote Sensing *Manual of Remote Sensing*; Colwell, 1983)

Name	Symbol	Units	Concept
Radiant energy	Q_λ	Joules, J	Capacity of radiation within a specified spectral band to do work
Radiant flux	Φ_λ	Watts, W	Time rate of flow of energy onto, off of, or through a surface
Radiant flux density at the surface			
Irradiance	E_λ	Watts per square meter $W\ m^{-2}$	Radiant flux incident upon a surface per unit area of that surface
Radiant exitance	M_λ	Watts per square meter $W\ m^{-2}$	Radiant flux leaving a surface per unit area of that surface
Radiance	L_λ	Watts per square meter per steradian $W\ m^{-2}\ sr^{-1}$	Radiant intensity per unit of projected source area in a specified direction
Hemispherical reflectance	r_λ	dimensionless	$\frac{\Phi_{reflected}}{\Phi_{i_\lambda}}$
Hemispherical transmittance	τ_λ	dimensionless	$\frac{\Phi_{transmitted}}{\Phi_{i_\lambda}}$
Hemispherical absorptance	α_λ	dimensionless	$\frac{\Phi_{absorbed}}{\Phi_{i_\lambda}}$

about the absorption and transmittance of the radiant energy. But because many of the sensor systems such as cameras and some multispectral scanners only record reflected energy, this information is still quite valuable and can form the basis for object identification and assessment. For example, it is clear from Figure 2-17 that grass reflects only approximately 15 percent of the incident red radiant energy (0.6 – 0.7 µm) while reflecting approximately 50 percent of the incident near-infrared radiant flux (0.7 – 0.9 µm). If we wanted to discriminate between grass and artificial turf, the ideal portion of the spectrum to remotely sense in would be the near-infrared region because artificial turf reflects only about 5 percent of the incident near-infrared energy. This would cause a black-and-white infrared image of the terrain to display grass in bright tones and the artificial turf in darker tones.

Hemispherical reflectance, transmittance, and absorptance radiometric quantities do not provide information about the exact amount of energy reaching a specific area on the ground from a specific direction or about the exact amount of radiant flux exiting the ground in a certain direction. Remote sensing systems can only be located in space at a single point in time, and they usually only look at a relatively small portion of the Earth at a single instant. Therefore, it is important to refine our radiometric measurement techniques so that more precise radiometric information can be extracted from the remotely sensed data. This requires the introduction of several radiometric quantities that provide progressively more precise radiometric information.

Radiant Flux Density

A flat area (e.g., 1 x 1 m in dimension) being bathed in radiant flux (Φ) in specific wavelengths from the Sun is shown in Figure 2-18. The amount of radiant flux intercepted divided by the area of the plane surface is the average *radiant flux density.*

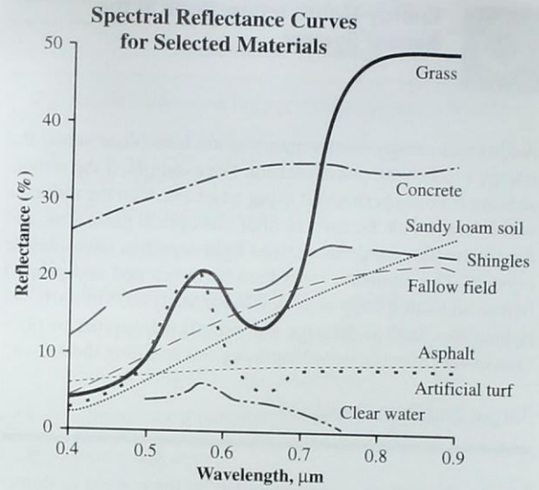

Figure 2-17 Typical spectral reflectance curves for urban-suburban phenomena in the region 0.4 – 0.9 µm (Jensen, 1989).

Irradiance and Exitance

The amount of radiant flux incident per unit area of a plane surface is called *irradiance* (E_λ):

$$E_\lambda = \frac{\Phi_\lambda}{A}. \qquad (2\text{-}19)$$

The amount of radiant flux leaving per unit area of the plane surface is called *exitance* (M_λ):

$$M_\lambda = \frac{\Phi_\lambda}{A}. \qquad (2\text{-}20)$$

Both quantities are usually measured in Watts per meter squared ($W\ m^{-2}$). Although we do not have information on the direction of either the incoming or outgoing radiant energy (i.e., the energy can come and go at any angle throughout the entire hemisphere), we have now refined the measurement to include information about the size of the study area of interest on the ground in m^2. Next we need to refine our radiometric measurement techniques to include information on what direction the radiant flux is leaving the study area.

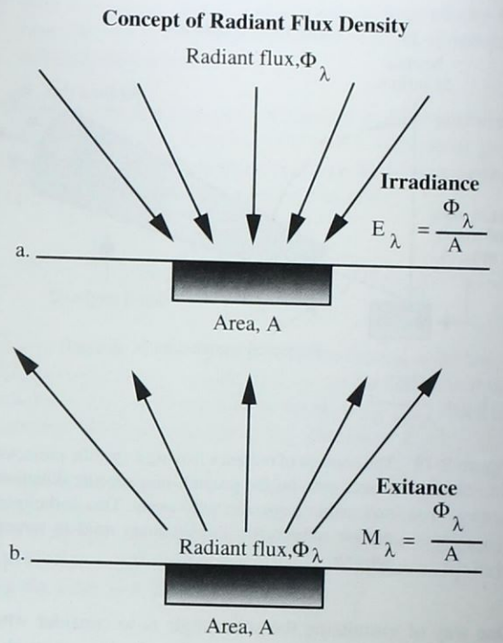

Figure 2-18 The concept of radiant flux density for an area on the surface of the Earth. a) *Irradiance* is a measure of the amount of incident energy in Watts m^{-2}. b) *Exitance* is a measure of the amount of energy leaving in Watts m^{-2}.

Radiance

Radiance is the most precise remote sensing radiometric measurement. *Radiance* (L_λ) is the radiant flux per unit solid angle leaving an extended source in a given direction per unit of projected source area in that direction. It is measured in Watts per meter squared per steradian ($W\ m^{-2}\ sr^{-1}$). The concept of radiance is best understood by evaluating Figure 2-19. First, the radiant flux leaves the projected source area in a specific direction toward the remote sensor. We are not concerned with any other radiant flux that might be leaving the source area in any other direction. We are only interested in the radiant flux in certain wavelengths (L_λ) leaving the projected source area within a certain direction ($A \cos \theta$) and solid angle (Ω):

$$L_\lambda = \frac{\frac{\theta}{\Omega}}{A \cos \theta}. \qquad (2\text{-}21)$$

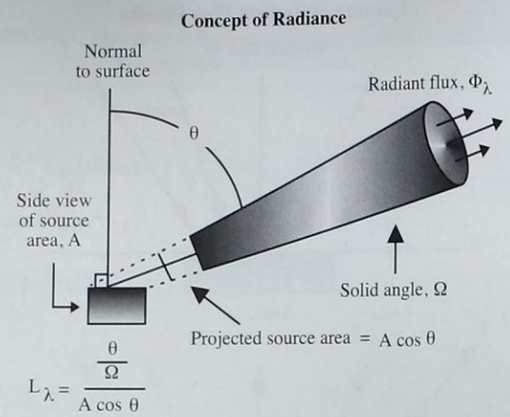

Figure 2-19 The concept of radiance leaving a specific projected source area on the ground, in a specific direction, and within a specific solid angle. This is the most precise radiometric measurement used in remote sensing.

One way of visualizing the solid angle is to consider what you would see if you were in an airplane looking through a telescope at the ground. Only the energy that exited the terrain and came up to and through the telescope in a specific solid angle (measured in steradians) would be intercepted by the telescope and viewed by your eye. Therefore, the solid angle is like a three-dimensional cone (or tube) that funnels radiant flux from a specific point source on the terrain toward the sensor system. Hopefully, energy from the atmosphere or other terrain features does not become scattered into the solid angle field of view and contaminate the radiant flux from the area of interest on the ground. Unfortunately, this is not often the case as scattering in the atmosphere and from other nearby areas on the ground can contribute spurious spectral energy which enters into the solid angle field of view.

Energy-Matter Interactions in the Atmosphere Once Again

The radiant flux reflected or emitted from the Earth's surface once again enters the atmosphere, where it interacts with the various gases, water vapor, and particulates. Thus, atmospheric scattering, absorption, reflection, and refraction influence the radiant flux once again before the energy is recorded by the remote sensing system.

Energy-Matter Interactions at the Sensor System

Additional energy-matter interactions take place when the energy reaches the remote sensor. For example, if the remote sensing is being performed using a camera, then the radiance will interact with the camera filter, the optical glass lens, and finally the film emulsion with its light-sensitive silver-halide crystals. The emulsion must then be developed and printed before an analog copy is available for analysis. Similarly, an optical-mechanical detector will record the number of photons in very specific wavelength regions reaching the sensor.

Target and Path Radiance

Ideally, the radiant energy recorded by the camera or detector is a true function of the amount of radiance leaving the terrain within the instantaneous field of view (IFOV) at a specific solid angle. Unfortunately, other radiant energy may enter into the field of view from various other paths and introduce confounding noise into the remote sensing process. More refined radiometric variable definitions are needed to identify the major sources and paths of this energy (Table 2-5). The various paths and factors that determine the radiance reaching the satellite sensor are summarized in Figure 2-20:

- *Path 1* contains spectral solar irradiance (E_{o_λ}) that was attenuated very little before illuminating the terrain within the IFOV. Notice in this case that we are interested in the solar irradiance from a specific solar zenith angle (θ_o) and that the amount of irradiance reaching the terrain is a function of the atmospheric transmittance at this angle (T_{θ_o}). If all of the irradiance makes it to the ground, then the atmospheric transmittance (T_{θ_o}) equals one. If none of the irradiance makes it to the ground, then the atmospheric transmittance is zero.

- *Path 2* contains spectral diffuse sky irradiance (E_{d_λ}) that never even reaches the Earth's surface (the study area) because of scattering in the atmosphere. Unfortunately, such energy is often scattered directly into the IFOV of the sensor system. As previously discussed, Rayleigh scattering of blue light contributes much to this diffuse sky irradiance. That is why the blue band image produced by a remote sensor system is often much brighter than any of the other bands. It contains much unwanted diffuse sky irradiance that was inadvertently scattered into the IFOV of the sensor system. Therefore, if possible, we want to minimize its effects.

Table 2-5. Fundamental Radiometric Variables

Radiometric Variables
E_o = solar irradiance at the top of the atmosphere (W m^{-2})
E_{o_λ} = spectral solar irradiance at the top of the atmosphere (W m^{-2} μm^{-1})
E_d = diffuse sky irradiance (W m^{-2})
E_{d_λ} = spectral diffuse sky irradiance (W m^{-2} μm^{-1})
E_g = global irradiance incident on the surface (W m^{-2})
E_{g_λ} = spectral global irradiance on the surface (W m^{-2} μm^{-1})
τ = normal atmospheric optical thickness
T_θ = atmospheric transmittance at an angle θ to the zenith
θ_o = solar zenith angle
θ_v = view angle of the satellite sensor (or scan angle)
μ = cos θ
r_λ = average target reflectance at a specific wavelength
r_{λ_n} = average reflectance from a neighboring area
L_s = total radiance at the sensor (W m^{-2} sr^{-1})
L_t = total radiance from the target of interest toward the sensor (W m^{-2} sr^{-1})
L_i = intrinsic radiance of the target (W m^{-2} sr^{-1}) (i.e., what a handheld radiometer would record on the ground without any intervening atmosphere)
L_p = path radiance from multiple scattering (W m^{-2} sr^{-1})

- *Path 3* contains energy from the Sun that has undergone some Rayleigh, Mie, and/or Non-selective scattering and perhaps some absorption and reemission before illuminating the study area. Thus, its spectral composition and polarization may be somewhat different than the energy that reaches the ground from Path 1.

- *Path 4* contains radiation that was reflected or scattered by nearby terrain (r_{λ_n}) covered by snow, concrete, soil, water, and/or vegetation into the IFOV of the sensor system. The energy does not actually illuminate the study area of interest. Therefore, if possible, we would like to minimize its effects.

- *Path 5* is energy that was also reflected from nearby terrain into the atmosphere, but then scattered or reflected onto the study area.

Therefore, for a given spectral interval in the electromagnetic spectrum (e.g., λ_1 to λ_2 could be 0.5 – 0.6 μm or green light), the total solar irradiance reaching the *Earth's surface*, E_{g_λ}, is an integration of several components:

$$E_{g_\lambda} = \int_{\lambda_1}^{\lambda_2} (E_{o_\lambda} T_{\theta_o} \cos\theta_o + E_{d_\lambda}) d\lambda \quad (\text{W m}^{-2}\,\mu\text{m}^{-1}) \quad (2\text{-}22)$$

It is a function of the spectral solar irradiance at the top of the atmosphere (E_{o_λ}) multiplied by the atmospheric transmittance (T_{θ_o}) at a certain solar zenith angle (θ_o) plus the contribution of spectral diffuse sky irradiance (E_{d_λ}).

Only a small amount of this irradiance is actually reflected by the terrain in the direction of the satellite sensor system. If we assume the surface of Earth is a diffuse reflector (a Lambertian surface), the total amount of radiance (L_T) exiting the study area toward the sensor is:

$$L_T = \frac{1}{\pi} \int_{\lambda_1}^{\lambda_2} r_\lambda T_{\theta_v} (E_{o_\lambda} T_{\theta_o} \cos\theta_o + E_{d_\lambda}) d\lambda \quad (2\text{-}23)$$

The average target reflectance factor (r_λ) is included because the vegetation, soil, and water within the IFOV selectively absorb some of the incident energy. Therefore, not all of the energy incident to the IFOV (E_{g_λ}) leaves the IFOV. In effect, the terrain acts like a filter, selectively absorbing certain wavelengths of light while reflecting others. Note that the energy exiting the terrain is at an angle (θ_v), requiring the use of T_{θ_v} in the equation.

It would be wonderful if the total radiance recorded by the sensor, L_s, equaled the radiance returned from the study area of interest, L_t. Unfortunately, $L_s \neq L_t$ because there is some additional radiance from different *paths* that may fall within the IFOV of the sensor system detector (Figure 2-20). This is often called *path radiance*, L_p. Thus, the total radiance recorded by the sensor becomes:

$$L_s = L_t + L_p \quad (\text{W m}^{-2}\,\text{sr}^{-1}). \quad (2\text{-}24)$$

We see from Equation 2-24 and Figure 2-20 that the path radiance (L_p) is an intrusive (bad) component of the total amount of radiance recorded by the sensor system (L_s). It is composed of radiant energy primarily from the diffuse sky irradiance (E_d) from path 2 as well as the reflectance from nearby

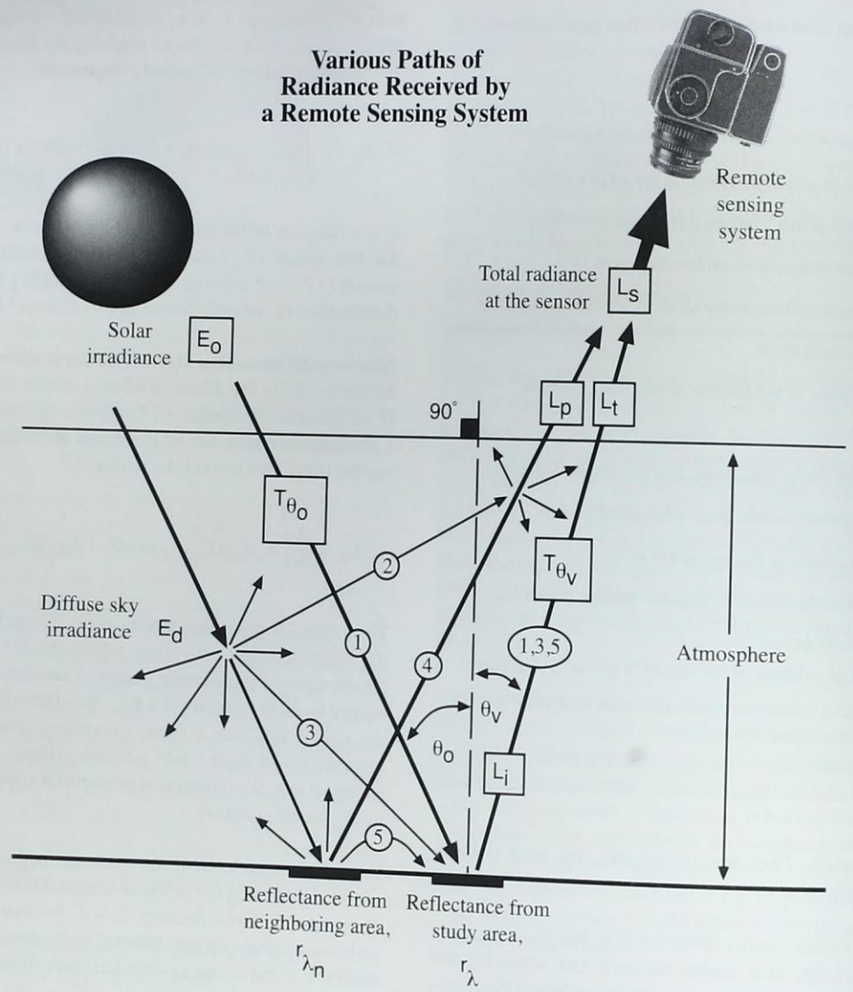

Figure 2-20 *Radiance* (L_t) from paths 1, 3, and 5 contains intrinsic valuable spectral information about the target of interest. Conversely, the *path radiance* (L_p) from paths 2 and 4 includes diffuse sky irradiance or radiance from neighboring areas on the ground. This path radiance generally introduces unwanted radiometric noise in the remotely sensed data and complicates the image interpretation process.

ground areas r_{λ_n} from path 4. Path radiance introduces error to the remote sensing data-collection process. It can impede our ability to obtain accurate spectral measurements.

A great deal of research has gone into developing methods to remove the contribution of path radiance (L_p). The methods usually require digital image processing and as such are beyond the scope of this text. However, several atmospheric correction methods are discussed in the chapter on Preprocessing in the companion book *Introductory Digital Image Processing* (Jensen, 1996). Also, commercial firms provide software that can be used to compute the atmospheric transmission and path radiance on a given day (Ontar, 1999). Such information can then be used to remove the path radiance (L_p) contribution to the remote sensing signal (L_S). The models require some atmospheric data that are hopefully available from nearby weather stations.

Conclusion

A scientist or lay person using remote sensing technology should understand the nature of the interactions taking place from the time that electromagnetic energy is created until it is recorded in analog or digital form by the remote sensing system (Duggin and Robinove, 1990). This knowledge increases the probability of accurate image interpretation and the extraction of valuable biophysical information from the imagery.

References

Bolemon, J., 1985, *Physics: An Introduction,* Englewood Cliffs, NJ: Prentice-Hall, Inc., 628 pp.

Clark, R. N., 1999, "Spectroscopy of Rocks and Minerals, and Principles of Spectroscopy," *Manual of Remote Sensing - Remote Sensing for the Earth Sciences*, A. N. Rencz (Ed.), NY: John Wiley & Sons, 672 pp.

Colwell, R. N., (Ed.), 1983, *Manual of Remote Sensing*, 2nd Ed., Falls Church: American Society of Photogrammetry, 2440 pp.

Duggin, M. J. and C. J. Robinove, 1990, "Assumptions Implicit in Remote Sensing Data Acquisition and Analysis," *International Journal of Remote Sensing*, 11(10):1669–1694.

Egan, W. G., 1985, *Photometry and Polarization in Remote Sensing*, NY: Elsevier, 503 pp.

Englert, B., M. O. Scully and H. Walther, 1994, "The Duality in Matter and Light," *Scientific American*, 271(6):86–92.

Feinberg, G., 1985, "Light," *The Surveillant Science: Remote Sensing of the Environment*, 2nd Ed., R. K. Holz (Ed.), NY: John Wiley & Sons, 2–11.

Jensen, J. R., (Ed.), 1989, "Remote Sensing in America," *Geography in America*, NY: Bobs Merrill, Inc., 746–775.

Jensen, J. R., 1996, *Introductory Digital Image Processing: A Remote Sensing Perspective*, Saddle River, NJ: Prentice-Hall, 318 pp.

Lousma, J. R., 1993, "Rising to the Challenge: The Role of the Information Sciences," *Photogrammetric Engineering & Remote Sensing*, 59(6):957–959.

Meadows, J., 1992, *The Great Scientists*, NY: Oxford University Press, 248 pp.

Mulligan, J. R., 1980, *Practical Physics: The Production and Conservation of Energy*, NY: McGraw-Hill, Inc., 526 pp.

Nassau, K., 1983, *The Physics and Chemistry of Color: The Fifteen Causes of Color*, NY: John Wiley & Sons.

Nassau, K., 1984, "The Physics of Color," in *Science Year 1984*, Chicago: World Book, 126–139.

Ontar, *1999 Product Catalog: PcModWin*, (commercial version of the U.S. Air Force Research Lab's MODTRAN), Andover: Ontar Inc., 23 pp.

Rinker, J. N., 1999, *Introduction to Spectral Remote Sensing*, Alexandria, VA: U.S. Army Topographic Engineering Center, http://www.tec.army.mil/terrain/desert/tutorial.

Sagan, C., 1994, *Pale Blue Dot*, NY: Random House, 429 pp.

Slater, P. N., 1980, *Remote Sensing: Optics and Optical Systems*, Reading, Pennsylvania: Addison-Wesley Publishing Company, 575 pp.

Strahler, A. N. and A. H. Strahler, 1989, *Elements of Physical Geography*, 4th Ed., NY: John Wiley & Sons, 562 pp.

Trefil, J. and R. M. Hazen, 1995, *The Sciences: An Integrated Approach*, NY: John Wiley & Sons, 634 pp.

Wolff, R. S. and L. Yaeger, 1993, *Visualization of Natural Phenomena*, Santa Clara, CA: Springer-Verlag, 374 pp.